The phylogenetic affinities of the bizarre Late Cretaceous Romanian theropod *Balaur bondoc* (Dinosauria, Maniraptora): dromaeosaurid or flightless bird?

Andrea Cau, Tom Brougham, Darren Naish

The exceptionally well-preserved Romanian dinosaur *Balaur bondoc* is the most complete theropod known to date from the Upper Cretaceous of Europe. Previous studies of this remarkable taxon have included its phylogenetic interpretation as an aberrant dromaeosaurid with velociraptorine affinities. However, *Balaur* displays a combination of both apparently plesiomorphic and derived bird-like characters. Here, we analyse those features in a phylogenetic revision and show how they challenge its referral to Dromaeosauridae. Our reanalysis of two distinct phylogenetic datasets focusing on basal paravian taxa supports the reinterpretation of *Balaur* as an avialan more crownward than *Archaeopteryx* but outside of Pygostylia, and as a flightless taxon within a paraphyletic assemblage of long-tailed birds. Our placement of *Balaur* within Avialae is not biased by character weighting. The placement among dromaeosaurids resulted in a suboptimal alternative that cannot be rejected based on the data to hand. Interpreted as a dromaeosaurid, *Balaur* has been assumed to be hypercarnivorous and predatory, exhibiting a peculiar morphology influenced by island endemism. However, a dromaeosaurid-like ecology is contradicted by several details of *Balaur*'s morphology, including the loss of a third functional manual digit, the non-ginglymoid distal end of metatarsal II, and a non-falciform ungual on the second pedal digit that lacks a prominent flexor tubercle. Conversely, an omnivorous ecology is better supported by *Balaur*'s morphology and is consistent with its phylogenetic placement within Avialae. Our reinterpretation of *Balaur* implies that a superficially dromaeosaurid-like taxon represents the enlarged, terrestrialised descendant of smaller and probably volant ancestors.

2 **The phylogenetic affinities of the bizarre Late Cretaceous Romanian theropod**

3 ***Balaur bondoc* (Dinosauria, Maniraptora): dromaeosaurid or flightless**

4 **bird?**

6 Andrea Cau[1]*, Tom Brougham[2, 3], Darren Naish[2, 3]

7 [1] Earth, Life and Environmental Sciences Department, Alma Mater Studiorum, Bologna

8 University, Italy; email: cauand@gmail.com;

9 [2] Ocean and Earth Science, University of Southampton, Southampton SO14 3ZH, UK; emails:

10 tbrougham@paravian.net, eotyrannus@gmail.com

11 [3] These authors contributed equally

12 *Corresponding author

15 The theropod dinosaur *Balaur bondoc* from the Maastrichtian (latest Late Cretaceous) of

16 Romania represents the most complete theropod dinosaur yet known from the Upper Cretaceous

17 of Europe (Csiki et al. 2010). The remarkably well-preserved holotype specimen of *B. bondoc*,

18 EME (Transylvanian Museum Society, Dept. of Natural Sciences, Cluj-Napoca, Romania)

19 PV.313, was collected from red overbank floodplain sediments of the Maastrichtian Sebeş

20 Formation in 2009 and comprises an articulated partial postcranial skeleton of a single

21 individual, including dorsal, sacral and caudal vertebrae as well as much of the pectoral and

22 pelvic girdles and limbs (Brusatte et al. 2013). The first phylogenetic studies incorporating

23 *Balaur* concluded that it represents an aberrant dromaeosaurid with velociraptorine affinities,

24 endemic to the European palaeoislands of the Late Cretaceous (Csiki et al. 2010; Turner et al.

25 2012; Brusatte et al. 2013). The matrices utilised in these three studies have all been versions of

26 the Theropod Working Group (TWiG) matrix, an incrementally and independently developed

27 large-scale matrix focusing on the interrelationships of coelurosaurian taxa (e.g., Norell et al.

28 2001; Makovicky et al. 2005; Turner et al. 2007; Turner et al. 2012; Brusatte et al. 2014).

29 Comparison made between *Balaur* and other dromaeosaurids reveals the possession of a suite of

30 autapomorphies not present in dromaeosaurids nor in most other non-avialan theropods, such as

31 a fused carpometacarpus, loss of a functional third manual digit, proximal fusion of the

32 tarsometatarsus, and a relatively enlarged first pedal digit (Csiki et al. 2010; Brusatte et al. 2013).

33 Interpreted as a dromaeosaurid, *Balaur* is a strikingly odd and apparently avialan-like taxon.

34 Recently, Godefroit et al. (2013a) included *Balaur* in a new phylogenetic analysis focusing on

35 paravians and found it resolved as a basal avialan, more crownward than *Archaeopteryx*. A

36 similar result was obtained independently by Foth et al. (2014) using a dataset expanded from

37 that of Turner et al. (2012): Foth et al. (2014) recovered *Balaur* in a position relatively less

38 crownward than in the tree obtained by Godefroit et al. (2013a), but still crownward of

39 *Archaeopteryx*. The present study focuses on resolving these conflicting interpretations regarding

40 the affinities of *Balaur* following examination of the holotype material (performed by TB and

41 DN). We also present a revised phylogenetic hypothesis based on a comparison of updated

42 versions of previously published taxon-character matrices.

43 **Materials and methods**

44 In order to test the competing dromaeosaurid and avialan hypotheses for the affinities of *Balaur*,

45 we coded the holotype specimen into modified versions of two recently published theropod

46 phylogenetic matrices: Brusatte et al. (2014) and Lee et al. (2014). Both of these large-scale and

47 independently coded matrices focused on the interrelationships of theropod dinosaurs and

48 contain a broadly overlapping and comprehensive sampling of over 100 theropod taxa (152 and

49 120 taxa respectively), including many basal avialans. The two matrices differ from each other in

50 the logical basis on character statement definitions (Sereno 2007; Brazeau 2011, see discussion

51 below).

52 *Brusatte et al. (2014) data set*

53 The dataset used by Brusatte et al. (2014) is an updated version of the dataset of Turner et al.

54 (2012). We modified the Brusatte et al. (2014) matrix for this study to include seven new

55 characters and updated character states for three previously defined characters (see Electronic

56 Supplementary Material). All character statements considered to be ordered by Brusatte et al.

57 (2014) were set accordingly. The resulting data matrix (860 characters vs 152 taxa) was then

58 analysed using the Hennig Society version of TNT v1.1 (Goloboff et al. 2008b; see Electronic

59 Supplementary Material for further details regarding modifications to the matrix and tree search

60 strategy).

61 *Lee et al. (2014) data set*

62 The dataset used by Lee at al. (2014) is an updated version of the dataset of Godefroit et al.

63 (2013a). Character statements of the 1549 included characters and the source of scores for the

64 included 120 fossil taxa are stored at the Dryad Digital Repository (Cau et al. 2014). In our

65 study, this dataset has been expanded to including an additional taxonomic unit based on the

66 extant avian *Meleagris* (ACUB 4817); accordingly, character statement 318 has been modified

67 (see Electronic Supplementary Material). *Balaur* was re-scored based on our examination of the

68 specimen and the incorporation of information from Brusatte et al. (2013). Lee et al. (2014)

69 applied Bayesian inference in their analysis of this dataset and integrating the morphological

70 information with chronostratigrafic information. In the present study, the updated morphological

71 data matrix (1549 characters vs 121 taxa) was analysed using parsimony as the tree search

72 strategy in TNT (see Electronic Supplementary Material).

73 *Alternative placement test and implied weighting analyses*

74 In our analyses of both datasets, we constrained the alternative deinonychosaurian and avialan

75 positions for *Balaur*, measuring step changes between resultant topologies as a further indication

76 of their relative support. Templeton's test (Templeton 1983) was used to determine whether the

77 step differences between the unforced and forced topologies were statistically significant. The

78 backbone constraints used the following species: a crown avian (*Anas platyrhynchus* in the

79 dataset of Brusatte et al. 2014, *Meleagris gallopavo* in the dataset of Lee et al. 2014), a

80 dromaeosaurid (*Dromaeosaurus albertensis* in both datasets), and a troodontid (*Troodon*

81 *formosus* in both datasets).

82 In order to test whether assumptions on downweighting of homoplasious characters influence the

83 placement of *Balaur* among Paraves, both datasets were subjected to implied weighting analyses

84 (IWAs, Goloboff 1993, Goloboff et al. 2008a, b; see Electronic Supplementary Material).

85 *Institutional abbreviations*

86 *ACUB*, Museo di Anatomia Comparata, University of Bologna, Bologna, Italy. *EME*,

87 Transylvanian Museum Society, Dept. of Natural Sciences, Cluj-Napoca, Romania.

88 **Comparative anatomy of *Balaur* and other maniraptoran theropods**

89 Compared to other theropods, *Balaur* displays a unique and unexpected combination of

90 characters (Brusatte et al. 2013). The phylogenetic analyses of Csiki et al. (2010) and Turner et

91 al. (2012) resolved *Balaur* as a velociraptorine dromaeosaurid. Consequently, most of the

92 unusual characters shared by *Balaur* with non-dromaeosaurid theropods were interpreted as

93 autapomorphies, independently evolved along the lineage leading exclusively to *Balaur*. An

94 alternative explanation is that these features may indicate a closer relationship between *Balaur*

95 and another non-dromaeosaurid clade of maniraptorans. Here, we list the most relevant

96 characters that may support or challenge the alternative placements of *Balaur* within

97 Maniraptora.

98 *Dorsal vertebrae with stalked parapophyses*

99 The dorsal vertebrae of *Balaur* bear distinctly stalked parapophyses (Brusatte et al. 2013).

100 Although this feature has been reported as a deinonychosaurian synapomorphy (Turner et al.

101 2012), stalked parapophyses are also present in alvarezsaurids and basal avialans (Novas 1997;

102 Chiappe et al. 1999; Agnolín and Novas 2013).

103 *Sacrum including at least seven fused vertebrae*

104 The presence of five fused sacral vertebrae is the plesiomorphic condition within coelurosaurs

105   (e.g., Brochu 2003). An independent increase in the number of fused sacral vertebrae is a

106   widespread phenomenon within Maniraptoriformes. Six to seven sacral vertebrae are present in

107   ornithomimids (Osmólska et al. 1972), Late Cretaceous oviraptorosaurs (Barsbold et al. 2000),

108   and some dromaeosaurids (Norell and Makovicky 1997; Turner et al. 2012; S. Brusatte pers.

109   comm. 2014). The synsacrum is composed of seven vertebrae in parvicursorine alvarezsauroids,

110   whereas in basal taxa it includes only five vertebrae (Choiniere et al. 2010). *Archaeopteryx* and

111   basal paravians retain five sacral vertebrae (Hwang et al. 2002; Paul 2002; Godefroit et al.

112   2013b; Godefroit et al. 2013a), whereas a sacrum with at least seven vertebrae has been regarded

113   as a synapomorphy of *Jixiangornis* and pygostylians (Turner et al. 2012). *Balaur* has at least

114   seven sacral vertebrae: four fused and clearly discernible sacral vertebrae bearing sacral ribs are

115   followed by three additional and co-ossified caudosacrals (Brusatte et al. 2013).

116   *Fused scapulocoracoid*

117   In *Balaur*, the scapula and coracoid are co-ossified and the suture is obliterated on both sides

118   (Fig. 1a; Brusatte et al. 2013). Brusatte et al. (2013) noted that a fused scapulocoracoid is present

119   in some dromaeosaurids (e.g., *Adasaurus*, *Microraptor*, *Velociraptor*; see Fig. 1c) but not in

120   others (e.g., *Achillobator*, *Buitreraptor*, *Deinonychus*, *Sinornithosaurus*, *Unenlagia*). Turner et

121   al. (2012) included fusion of the scapulocoracoid among the phylogenetically informative

122   characters of their paravian phylogeny. Within non-avialan coelurosaurs, the presence of this

123   character state has been reported within ornithomimosaurs, therizinosauroids, alvarezsauroids,

124   tyrannosaurids and oviraptorosaurs (Osmólska et al. 1972; Perle 1979; Perle et al. 1994; Brochu

125   2003; Balanoff and Norell 2012), suggesting a high degree of homoplasy. Fusion of the

126   scapulocoracoid is also present in basal avialans (e.g., Confuciusornithidae; Chiappe et al. 1999)

127   and flightless avians (e.g., *Struthio*; ACUB 4820).

128   *Coracoid with prominent tuber placed on the anterolateral corner*

129   The coracoid of *Balaur* bears a hypertrophied tubercle that forms the anterolateral corner of the

130   bone and obscures the supracoracoid nerve foramen when the coracoid is observed in lateral

131   view (Fig. 1a; Brusatte et al. 2013). Non-avialan theropods possess tubercles that are relatively

132   smaller and more lateroventrally directed (when the scapula is oriented horizontally) than that

133   seen in avialan theropods (Fig. 1c; Osmólska et al. 1972; Ostrom 1976; this is the "*processus*

134   *praeglenoidalis*" *sensu* Elzanowski et al. 2002). Although the coracoid tubercle of *Balaur* may

135 appear autapomorphic among non-avialan theropods (Brusatte et al. 2013), a prominent coracoid

136 tubercle is also present in unenlagiines (*Buitreraptor*, see Agnolin and Novas 2013), basal

137 avialans (e.g., *Jeholornis*, *Jixiangornis*; Turner et al. 2012, fig. 82), and forms the acrocoracoid

138 of ornithothoracines (e.g., *Apsaravis*, *Enantiophoenix*, *Enantiornis*; Clarke and Norell 2002;

139 Baier et al. 2007; Cau and Arduini 2008; Walker and Dyke 2009; Fig. 1). A hypertrophied

140 coracoid tubercle that obscures the supracoracoid nerve foramen in lateral view is also seen in

141 *Sapeornis* (Zhou and Zhang 2003; Gao et al. 2012).

142 *Humerus longer than half the combined length of tibiotarsus and tarsometatarsus*

143 The ratio between the lengths of the humerus and femur is usually considered as a

144 phylogenetically informative character in discussions on the evolution of coelurosaurian

145 theropods (e.g., Brusatte et al. 2014, character 262), as that ratio is usually higher among

146 avialans than it is in most non-avialan theropods. Since the femur of *Balaur* is unknown

147 (Brusatte et al. 2013), we used the ratio between the length of the humerus and the sum of the

148 lengths of the tibiotarsus and tarsometatarsus. The humerus of non-avialan theropods is

149 consistently shorter than half the combined length of the tibiotarsus and tarsometatarsus (e.g.,

150 *Deinonychus*, *Gallimimus*, *Microraptor*, *Tyrannosaurus*; Ostrom 1969; Osmólska et al. 1972;

151 Hwang et al. 2002; Brochu 2003). In *Balaur*, the humerus is longer than half the combined

152 length of the tibiotarsus and tarsometatarsus (55%) and approaches the condition seen in basal

153 avialans (e.g., *Archaeopteryx*: 59%, *Confuciusornis*: 67%, *Jeholornis*: 77%; Chiappe et al. 1999;

154 Elzanowski 2001; Zhou and Zhang 2002; see Brusatte et al. 2013, table 2). The interpretation of

155 this feature is problematic, since distal hindlimb elongation is not correlated to femur length

156 among theropods (Holtz 1995); accordingly, we have avoided its inclusion among the new

157 characters added to the phylogenetic analyses. We have retained the original humerus/femur

158 ratio characters in both datasets and thus score *Balaur* as "unknown" for them. Therefore, the

159 results of our analyses are not biased by the use of that character.

160 *Humeral condyles placed on the anterior surface of the distal end*

161 The humerus of *Balaur* possesses condyles that are placed entirely on the anterior surface of the

162 bone (Brusatte et al. 2013). As in *Balaur*, the complete anterior migration of the humeral

163 condyles is present in therizinosauroids (e.g., Zanno 2010), alvarezsauroids (Novas 1997), basal

164 pygostylians (e.g., *Confuciusornis*, *Limenavis*, *Enantiornis*; Chiappe et al. 1999; Clarke and

165 Chiappe 2001; Walker and Dyke 2009), and extant birds (e.g., *Dromaius*, *Meleagris*, *Struthio*;

166 ACUB 3131; 4817; 4820). All other known dromaeosaurids (e.g., *Deinonychus*; Ostrom 1969),

167 most non-avialan theropods (e.g., *Gallimimus*, *Allosaurus*, *Tyrannosaurus*; Osmólska et al. 1972;

168 Madsen 1976; Brochu 2003), and early avialans (e.g., *Archaeopteryx*; Berlin specimen) bear the

169 condyles in a more distal position, with a limited, if not absent, extent onto the anterior surface of

170 the bone. In the analysis of Turner et al. (2012), *Balaur* was scored as retaining the primitive

171 condition (*contra* Brusatte et al. 2013, 2014).

172 *Deep and elongate triangular brachial fossa on humerus*

173 The humerus of *Balaur* bears a prominent triangular fossa on the anterior surface of the distal

174 end of the humerus (Brusatte et al. 2013, fig. 12). This fossa is bordered both laterally and

175 medially by raised crests confluent with the epicondyles. The same configuration defines the

176 brachial fossa present in pygostylians (e.g., *Confuciusornis*, *Limenavis*, *Apsaravis*; Chiappe et al.

177 1999; Clarke and Chiappe 2001; Clarke and Norell 2002). This fossa is also variably developed

178 within dromaeosaurids (e.g., *Bambiraptor*; Turner et al. 2012; Brusatte et al. 2013).

179 *Ulna with brachial depression*

180 The proximal third of *Balaur*'s ulna bears a shallow, elongate depression on the medial surface

181 termed the "proximal fossa" (Brusatte et al. 2013, fig. 14). This character is topographically

182 equivalent to the brachial fossa present in pygostylians (Baumel and Witmer 1993; Clarke and

183 Chiappe 2001; Walker and Dyke 2009). The ulna of most non-avialan theropods lacks a brachial

184 depression or possesses a poorly developed one (e.g., *Allosaurus*, *Tyrannosaurus*; Madsen 1976;

185 Brochu 2003). However, the structure is well developed in some dromaeosaurids (e.g.,

186 *Bambiraptor*, *Buitreraptor*; Burnham 2004; Agnolín and Novas 2011; Agnolín and Novas 2013).

187 *Distal carpals fused to proximal end of metacarpals*

188 The manus of *Balaur* displays co-ossification of the distal carpals with the proximal ends of the

189 metacarpals (Fig. 2a; Brusatte et al. 2013), unlike the dromaeosaurid condition in which no such

190 fusion in present (Fig. 2d). The fusion between the distal carpals and the metacarpals is present

191 in a few non-avialan theropod lineages (e.g., *Avimimus*, *Mononykus*; Kurzanov 1981; Perle et al.

192 1993), and in pygostylians (e.g., *Confuciusornis*, *Xiangornis*; Chiappe et al. 1999; Hu et al.

193 2012). In particular, the pattern of proximal fusion among the carpometacarpal elements in

194 *Balaur* is shared by most basal pygostylians (e.g., *Confuciusornis*, *Sinornis*, *Sapeornis*,

195   *Pengornis, Enantiornis, Zhouornis*; Chiappe et al. 1999; Sereno et al. 2002; Zhou and Zhang

196   2003; Zhou et al. 2008; Walker and Dyke 2009; Zhang et al. 2013; see Fig. 2b-c, Fig. S1). Most

197   ornithurines and some enantiornithines display complete distal fusion between metacarpals II

198   and III in addition to the aforementioned proximal fusion of the carpometacarpus as seen in

199   *Balaur* (e.g., *Apsaravis, Teviornis, Xiangornis*; Clarke and Norell 2002; Kurochkin et al. 2002;

200   Hu et al. 2012).

201   *Semilunate carpal shifted laterally and first metacarpal sloped proximolaterally*

202   In *Balaur*, the semilunate carpal overlaps the whole proximal ends of both metacarpals II and III

203   (Fig. 2a, Fig. S1). Furthermore, the proximal end of the first metacarpal in *Balaur* is

204   mediolaterally narrower than the distal end, producing a proximolaterally sloping medial margin

205   of the metacarpus. In *Archaeopteryx* and most non-avialan maniraptorans, the proximal end of

206   the first metacarpal is not constricted compared to the distal end, and the semilunate carpal

207   overlaps most of metacarpal I; meanwhile, the overlap on metacarpal III is absent or limited to

208   the medialmost margin of the bone (Fig. 2d; Ostrom 1976, fig. 10; Xu et al. 2014). Therefore, the

209   position of the semilunate carpal of *Balaur* represents a lateral shift compared to the condition in

210   other non-avialan maniraptorans, and recalls long-tailed and pygostylian birds where the

211   semilunate carpal has a reduced or absent overlap on metacarpal I and extensively covers both

212   metacarpals II and III (e.g., *Confuciusornis, Sinornis, Sapeornis, Enantiornis, Zhouornis*;

213   Chiappe et al. 1999; Sereno et al. 2002; Zhou and Zhang 2003; Walker and Dyke 2009; Zhang et

214   al. 2013; see also Xu et al. 2014; see Fig. 2b-c). As in *Balaur*, pygostylian birds show a

215   mediolateral constriction of the proximal end of the first metacarpal, and a medial margin

216   ("anterior margin", using *Nomina Anatomica Avium* nomenclature, see Harris 2004) that is

217   variably sloped proximolaterally in extensor view.

218   *Condyles of metacarpals I-II restricted to the distal and ventral surfaces of the metacarpals*

219   Metacarpals I and II of *Balaur* bear condyles that are restricted to the distal and ventral surfaces

220   of the metacarpals, and are excluded from the extensor surfaces (Brusatte et al. 2013). The

221   dromaeosaurid condition (e.g., *Deinonychus, Velociraptor, Graciliraptor*; Ostrom 1969; Norell

222   and Makovicky 1999; Xu and Wang 2003), in which the condyles are expanded along the

223   extensor surface of the metacarpals, is present in most non-avialan theropods (e.g.,

224   *Acrocanthosaurus, Allosaurus, Australovenator, Berberosaurus, Dilophosaurus, Patagonykus*,

225 *Rapator*; Madsen 1976; Welles 1984; Novas 1997; Senter and Robins 2005; Allain et al. 2007;

226 White et al. 2013). The condition present in the metacarpals of *Balaur* is also present in

227 pygostylians (e.g., *Teviornis*, *Sinornis*, *Enantiornis*; Kurochkin et al. 2002; Sereno et al. 2002;

228 Walker and Dyke 2009) and extant avians (e.g., *Dromaius*; *Meleagris*, *Struthio*; ACUB 3131;

229 4817; 4820). Furthermore, the ventral surface of the metacarpals of *Balaur* are excavated by a

230 wide flexor sulcus but lack distinct flexor pits at the distal end, similar to the condition present in

231 avialans (e.g., *Teviornis*; Kurochkin et al. 2002) but differing from that of dromaeosaurids and

232 most non-avialan theropods that do bear a distinct flexor pit (e.g., *Allosaurus*, *Acrocanthosaurus*,

233 *Mahakala*, *Velociraptor*; Madsen 1976; Senter and Robins 2005; Turner et al. 2011).

234 *Metacarpal II with an intermetacarpal ridge running along the dorsolateral edge of the bone*
235 *and closed intermetacarpal space between metacarpals II and III*

236 *Balaur* possesses a distinct web of bone that extends along the dorsolateral edge of metacarpal II

237 and contacts metacarpal III distally, and a distally closed intermetacarpal space between

238 metacarpals II and III (Brusatte et al. 2013). Within basal avialans, the extent of the contact

239 between metacarpals II and III displays some variation, ranging from the close contact of a

240 straight metacarpal III to metacarpal II with no intermetacarpal space (e.g., *Sapeornis*; Zhou and

241 Zhang 2003; Gao et al. 2012; see Fig. 2, Fig. S1), an appressed distal contact but no fusion of

242 metacarpal III to metacarpal II (the condition as seen in *Balaur* and many basal avialans,

243 including *Jeholornis*, *Enantiornis*, *Confuciusornis*, *Zhouornis*, and *Piscivoravis*; Zhou and Zhang

244 2002; Walker and Dyke 2009; Zhang et al. 2009; Zhang et al. 2013; Zhou et al. 2014), to distal

245 obliteration of the contact between metacarpals II and III due to complete fusion between the

246 bones (e.g., *Teviornis*, *Xiangornis, Meleagris*; Kurochkin et al. 2002; Hu et al. 2012; ACUB

247 4817). A closed intermetacarpal space is present in *Confuciusornis* (Chiappe et al. 1999; Zhang

248 et al. 2009), some long-tailed birds (e.g., *Jeholornis*, *Jixiangornis*; Zhou and Zhang 2002), and

249 ornithothoracines (e.g., *Enantiornis*, *Xiangornis*, *Zhouornis*; Walker and Dyke 2009; Hu et al.

250 2012; Zhang et al. 2013; see Fig. 2b). Most euornithines differ from *Balaur* and most other

251 avialans in having a more distally placed intermetacarpal space relative to a more shortened

252 metacarpal I (e.g., *Teviornis*; Kurochkin et al. 2002).

253 *Distal end of metacarpal III unexpanded and not divided into separated condyles*
254 The third metacarpal of *Balaur* bears a simple distal end that lacks distinct condyles.

255   Dromaeosaurids share with most non-avialan theropods the presence of well-defined metacarpal

256   condyles separated by an intercondylar sulcus (e.g., *Allosaurus*, *Bambiraptor*, *Deinocheirus*,

257   *Deinonychus*, *Dilophosaurus*, *Gallimimus*; Ostrom 1969; Osmólska and Roniewicz 1970;

258   Osmólska et al. 1972; Madsen 1976; Welles 1984; Burnham 2004). The condition present in the

259   third metacarpal of *Balaur* is shared by tyrannosaurids (e.g., *Tyrannosaurus*; Lipkin and

260   Carpenter 2008, fig. 10.10), basal pygostylians (e.g., *Confuciusornis*, *Enantiornis*, *Sinornis*,

261   *Teviornis*, *Xiangornis, Zhouornis*; Chiappe et al. 1999; Kurochkin et al. 2002; Sereno et al. 2002;

262   Walker and Dyke 2009; Hu et al. 2012; Zhang et al. 2013) and crown avians (e.g., *Meleagris*,

263   *Struthio*; ACUB 4817; 4820). This character is not obviously linked with the reduction in the

264   number of phalanges in digit III (see below), since *Confuciusornis* shows the derived metacarpal

265   condition (i.e., simple distal end of metacarpal III) yet retains a full set of four functional

266   phalanges in digit III.

267   *Third manual digit bearing less than three phalanges*

268   The third manual digit of *Balaur* is extremely reduced and lacks the distal phalanges, including

269   the ungual (Fig. 2a; Brusatte et al. 2013). The only known phalanx in the third manual digit of

270   *Balaur* has a tapering distal end with a small distal articular surface, suggesting the presence of a

271   possible additional phalanx of very small size. Such a reduction is unknown in dromaeosaurids,

272   which have three non-ungual phalanges on manual digit III and a fully functional ungual (Fig.

273   2d), but it is commonly found in non-confuciusornithid pygostylians, where the third manual

274   digit is usually reduced to two or fewer phalanges, the most distal of which has a tapering distal

275   end and poorly defined articular surfaces (e.g., *Sinornis*, *Sapeornis*, *Zhouornis*, *Piscivoravis*;

276   Sereno et al. 2002; Gao et al. 2012; Zhang et al. 2013; Zhou et al. 2014; see Fig. 2b-c, Fig. S1).

277   *Dorsal margin of manual unguals does not arch dorsally above level of articular facet and flexor*

278   *tubercles not expanded ventrally*

279   Senter (2007a) argued that in dromaeosaurid manual unguals, the dorsal margins arch higher

280   than the articular facets when the latter is held vertically, and that this feature differentiates

281   dromaeosaurid manual unguals from those of other theropods. The derived condition is present

282   in microraptorines and eudromaeosaurs but is absent in unenlagiines (Senter 2007a; Senter

283   2007b; Currie and Paulina Carabajal 2012; Fig. S1A-B). Furthermore, the manual unguals in

284   both dromaeosaurids and troodontids bear prominent and dorsoventrally expanded flexor

285   tubercles. Following the method described by Senter (2007a), we note that the dorsal margins of

286   *Balaur*'s manual unguals do not arch higher than the articular facet, and that the flexor tubercles

287   are relatively low and more elongate proximodistally than they are deep dorsoventrally (Brusatte

288   et al. 2013 figs. 21-22, figs. 21-22; Fig. S1C). Similar absence of a markedly convex dorsal

289   margin of the manual ungual and relatively moderate development of the flexor tubercles is

290   widespread among the manual unguals of basal avialans (e.g., *Sinornis*, *Sapeornis*, *Zhouornis*,

291   *Piscivoravis*; Sereno et al. 2002; Gao et al. 2012; Zhang et al. 2013; Zhou et al. 2014; see Fig.

292   2b-c).

293   *Complete coossification of pelvic bones*

294   *Balaur* displays coossification of the pelvic bones such that both the iliopubic and ilioischial

295   sutures are obliterated (Brusatte et al. 2013, Fig. S2A). In most tetanuran theropods, including

296   basalmost avialans, the pelvic elements do not completely coossify (e.g., *Allosaurus*, *Jeholornis*,

297   *Patagonykus*, *Sapeornis*, *Tyrannosaurus*; Madsen 1976; Novas 1997; Zhou and Zhang 2002;

298   Brochu 2003; Zhou and Zhang 2003). This contrasts with ceratosaurian-grade theropods

299   (Tykoski and Rowe 2004), some non-avialan coelurosaurs (e.g., *Avimimus*; Kurzanov 1981) and

300   ornithothoracines (e.g., *Apsaravis*, cf. *Enantiornis*, *Patagopteryx*, *Qiliania*, *Sinornis*; Chiappe

301   2002; Chiappe and Walker 2002; Clarke and Norell 2002; Sereno et al. 2002; Ji et al. 2011, Fig.

302   S2D) in which the pelvic bones fuse completely. Although coossification of the ilium to the

303   pubis is present in the only known specimen of the microraptorine dromaeosaurid

304   *Hesperonychus*, the pelvic coossification differs from *Balaur* and avialans as the ilioischial

305   articulation remains unfused (Longrich and Currie 2009).

306   *Ridge bounding the cuppedicus fossa confluent with the acetabular rim*

307   In the ilium of *Balaur*, the ridge that dorsally bounds the cuppedicus fossa is extended

308   posteriorly on the lateral surface of the pubic peduncle and is confluent with the acetabular rim

309   (Brusatte et al. 2013; Fig. S2A). This feature is a compound character formed by the presence of

310   a ridge bounding the cuppedicus fossa, which is a neotetanuran synapomorphy (Hutchinson

311   2001; Novas 2004), and the posterior extension of the cuppedicus fossa on the lateral surface of

312   the pubic peduncle, which is a derived feature of paravians (Hutchinson 2001, figs. 4-6). The

313   combination of features present in *Balaur* is shared by *Anchiornis* and *Xiaotingia* (Turner et al.

314   2012), *Unenlagia* and *Rahonavis* (Novas 2004), *Velociraptor* (Norell and Makovicky 1999) and

315   enantiornithines (e.g., Sereno et al. 2002, fig. 8.4; Walker and Dyke 2009, Fig. S2D). The

316   presence and extent of the cuppedicus fossa is difficult to determine in most Mesozoic avialans

317   because of the two-dimensional preservation of most specimens (Novas 2004). Furthermore, the

318   character statements relative to the ridge bounding the cuppedicus fossa in phylogenetic analyses

319   are marked as 'inapplicable' in those taxa lacking a distinct cuppedicus fossa (Hutchinson 2001;

320   e.g., *Mahakala*, *Patagopteryx*, Ornithurae; Turner et al. 2011), a scoring strategy followed by

321   both Turner et al. (2012) and Godefroit et al. (2013a).

322   *Pubis and ischium projected strongly posteroventrally and subparallel*

323   *Balaur* has a posteroventrally directed pubis, subparallel to the ischium (Csiki et al. 2010; Fig.

324   S2A). Although Brusatte et al. (2013) acknowledged that the extreme posterior inclination of the

325   pubis may partially be the result of taphonomic distortion, they confirmed the genuine

326   posteroventral orientation of this bone. Within Theropoda, retroversion of the pubis

327   (opisthopuby) is known in therizinosauroids, parvicursorine alvarezsaurids, dromaeosaurids and

328   pygostylians. Most therizinosauroids (but not *Falcarius*) show a posteroventrally directed pubis

329   that articulates with the obturator process of the ischium (Zanno 2010). Opisthopuby is present in

330   many parvicursorines (e.g., *Mononykus*; Perle et al. 1994), but absent in more basal

331   alvarezsauroids (e.g., *Haplocheirus*, *Patagonykus*; Novas 1997; Choiniere et al. 2010). A

332   retroverted pubis is absent in basal paravians – they instead display a vertically oriented

333   ('mesopubic') pubis – and is present in some dromaeosaurids (e.g., *Adasaurus* and *Velociraptor*;

334   Norell and Makovicky 1999; Xu et al. 2010; Turner et al. 2012) but absent in others (e.g.,

335   *Achillobator*, *Utahraptor*; Perle et al. 1999; Senter et al. 2012). It is also a common feature in

336   pygostylian birds (e.g., *Confuciusornis*, *Patagopteryx*, *Sapeornis*; Chiappe et al. 1999;

337   Hutchinson 2001; Chiappe 2002; Chiappe and Walker 2002; Zhou and Zhang 2003).

338   *Broad pelvic canal with laterally convex pubes and abrupt distal narrowing of interpubic*

339   *distance*

340   Brusatte et al. (2013) noted as an autapomorphy of *Balaur* an interpubic distance that is

341   proportionally greater than that present in other dromaeosaurids (e.g., *Velociraptor*; Norell and

342   Makovicky 1997; Norell and Makovicky 1999). The gap between the laterally bowed pubes of

343   *Balaur* only begins to narrow abruptly in the distalmost third of the bone (Fig. 3b, Fig. S2B;

344   Brusatte et al. 2013, fig. 56). This condition differs from that seen in most theropods (e.g.,

345 *Avimimus*, *Sinraptor*, *Tyrannosaurus*; Currie and Zhao 1993; Vickers-Rich et al. 2002; Brochu

346 2003), including *Velociraptor* (Fig. 3d, Fig. S2C; Norell and Makovicky 1999; Brusatte et al.

347 2013), *Bambiraptor* (Burnham 2004) and *Archaeopteryx* (Norell and Makovicky 1999, fig. 25),

348 where the narrowing is more gradual over the length of the pubes and the pubis is not bowed

349 laterally in anteroposterior view. Brusatte et al. (2013) noted that the condition in *Balaur* is

350 somewhat similar to the condition in therizinosaurids (Zanno 2010). The combination of a

351 relatively broad pelvic canal, bounded by laterally convex pubes and with an abrupt distal

352 narrowing of the interpubic distance, is also seen in pygostylian birds (e.g., *Concornis*,

353 *Dapingfangornis*, *Piscivoravis*, *Sapeornis*, *Yanornis*; Sanz et al. 1995; Zhou and Zhang 2003; Li

354 et al. 2006; Zhou et al. 2014; Zheng et al. 2014; see Figs. 3c, Fig. S2E).

355 *Ischial tuberosity*

356 The ischium of *Balaur* bears a well-developed obturator tuberosity (*ischial tuberosity* of

357 Hutchinson 2001) on the dorsal end of the part of its anterior margin that contacts or nearly

358 contacts the pubis ventrally (Brusatte et al. 2013). This feature was determined to be a

359 synapomorphy of the velociraptorine subclade (including *Balaur*) by Turner et al. (2012).

360 However, almost all non-velociraptorine taxa were scored by them as either unknown for or

361 lacking an ischial tuberosity (char. 176 in Turner et al. 2012), with only *Adasaurus*, *Anchiornis*,

362 *Deinonychus* and *Velociraptor* scored as bearing that feature. Nevertheless, a prominent ischial

363 tuberosity is also present in avialans, in particular in large-bodied flightless taxa (e.g.,

364 *Patagopteryx*; Hutchinson 2001). The ischial tuberosity of some avialans approaches and

365 contacts the pubis (e.g., *Dromaius*; ACUB 3131), and is the case in *Balaur*.

366 *Ischium with proximodorsal flange*

367 The ischium of *Balaur* bears a process along the dorsal half of its dorsal surface (Brusatte et al.

368 2013, fig. 27A: "dorsal flange of proximal ischium"). This process is topographically equivalent

369 to the proximal dorsal ischial tuberosity of other reptiles (Hutchinson 2001). This structure is

370 variably developed on the ischia of many paravians (e.g., Novas and Puerta 1997; Forster 1998;

371 Xu et al. 1999; Agnolín and Novas 2013). In unenlagiines and microraptorines, the ischium bears

372 a tuber-like proximodorsal process (Novas and Puerta 1997; Agnolín and Novas 2013, figs. 3.5c-

373 e) which is absent in known velociraptorines (Norell and Makovicky 1999; Agnolín and Novas

374 2013; Brusatte et al. 2013) except for a *Velociraptor*-like taxon from Mongolia (Norell and

375 Makovicky 1999, fig 24). In basal avialans, the ischial tuberosity is developed as a prominent

376 trapezoidal flange which is more proximodistally expanded than it is in other paravians and

377 which resembles the condition present in *Balaur* (e.g., *Confuciusornis*, cf. *Enantiornis*,

378 *Jeholornis*, *Patagopteryx*, *Sapeornis*, *Sinornis*; Chiappe et al. 1999; Hutchinson 2001; Sereno et

379 al. 2002; Zhou and Zhang 2002; Zhou and Zhang 2003; Walker and Dyke 2009; see Agnolín and

380 Novas 2013; Fig. S2D, F).

381 *Fibula fused to tibia proximally*

382 In *Balaur*, the tibia and the fibula are fused proximally (Brusatte et al. 2013), a condition not

383 seen in dromaeosaurids or most non-avialan theropods. Among coelurosaurs, a more extensive

384 proximal fusion between tibia and fibula is present in pygostylian birds (e.g., *Qiliania*; Ji et al.

385 2011).

386 *Tuber and ridge along lateral surface of the distal end of the tibiotarsus*

387 The distal end of the tibiotarsus of *Balaur* bears a pronounced anteroposteriorly oriented lateral

388 ridge. The ridge is most pronounced anteriorly, where it terminates at a discrete rounded tubercle

389 located at the point where the lateral condyle and shaft merge. The ridge is kinked at its midpoint

390 where it forms a second, ventrally directed tubercle positioned laterodistally relative to the first

391 tubercle (Brusatte et al. 2013, fig. 35). Brusatte et al. (2013) suggested that the first tubercle may

392 represent the distal end of the fibula, fused to the tibiotarsus, whereas no interpretation of the

393 second tubercle was provided. A raised ridge along the anterolateral margin of the distal end of

394 the tibiotarsus at the point of fusion between the tibia and the proximal tarsals is also present in

395 *Qiliania* (Ji et al. 2011) and in the enigmatic Haţeg taxon *Bradycneme* (Harrison and Walker

396 1975). Based on comparison with birds, we interpret the second tubercle and the corresponding

397 kinked ridge as the fibular facet of the calcaneum. According to our interpretation, the other

398 (more proximally placed) tubercle is topographically equivalent to the *tuberculum retinaculi M.*

399 *fibularis* of birds (Baumel and Witmer 1993).

400 *Complete distal co-ossification of the tibiotarsus*

401 The distal end of the tibia and the proximal tarsals of *Balaur* are coossified, forming a tibiotarsus

402 where the sutures are obliterated (Brusatte et al. 2013). Turner et al. (2012) considered the fusion

403 between the calcaneum and astragalus, but not the tibia and tarsals, to be a synapomorphy of

404 Paraves. Fusion involving the proximal tarsals and the distal end of the tibia is a condition seen

405   in some basal neotheropods (Tykoski and Rowe 2004). Within non-avialan coelurosaurs,

406   coossification of the proximal tarsals and the distal end of the tibia is observed in alvarezsaurids

407   (e.g., *Albinykus*, *Mononykus*; Perle et al. 1994; Nesbitt et al. 2011) and some oviraptorosaurs

408   (e.g., *Avimimus*, *Elmisaurus*; Osmólska 1981; Vickers-Rich et al. 2002). Within Avialae, the

409   presence of a fully coossified tibiotarsus is present in taxa more crownward than *Archaeopteryx*

410   (e.g., *Apsaravis*, *Confuciusornis*, *Hollanda*; Chiappe et al. 1999; Clarke and Norell 2002; Bell et

411   al. 2010).

412   *Deep extensor groove on distal tibiotarsus*

413   *Balaur* bears a deep and prominent extensor groove on the distal end of the tibiotarsus (Brusatte

414   et al. 2013). Within dromaeosaurids, this feature has otherwise been reported only in

415   *Buitreraptor* and is homoplastically present in other maniraptoran lineages (e.g., *Apsaravis*,

416   *Hollanda*, *Mononykus*; Perle et al. 1994; Clarke and Norell 2002; Bell et al. 2010).

417   *Tibiotarsus with intercondylar sulcus extended along the posterior surface*

418   The distal end of *Balaur*'s tibiotarsus is saddle-shaped due to the presence of a large and distinct

419   intercondylar sulcus (Brusatte et al. 2013). The latter feature is restricted not only to the

420   anterodistal end of the bone but also extends along the distal end of the posterior surface as a

421   flexor sulcus. This feature is also present in basal avialans known from three-dimensionally

422   preserved specimens (e.g., *Apsaravis*, *Hollanda*; Clarke and Norell 2002; Bell et al. 2010).

423   *Deep circular pit on medial surface of distal tibiotarsus*

424   The medial surface of the distal end of *Balaur*'s tibiotarsus is excavated by a deep subcircular pit

425   which was described as being deeper than are the homologous depressions variably present in the

426   astragali of some dromaeosaurids (Brusatte et al. 2013). A pit comparable in depth to that present

427   in *Balaur* is also present in avialans more crownward than *Archaeopteryx* (*depressio*

428   *epicondylaris medialis*, Baumel and Witmer 1993) and has been considered a phylogenetically

429   informative feature (see O'Connor et al. 2011).

430   *Extensive coossification of tarsometatarsus*

431   The tarsometatarsal elements of *Balaur* display extensive coossification (Fig. 4a, Figs. S3-4;

432   Brusatte et al. 2013), in contrast to most non-avian theropods in which no such fusion is present

433   (e.g., *Velociraptor*; see Fig. 4b, Fig. S4A). Many maniraptoran lineages display coossification of

434   the distal tarsals to the proximal ends of the metatarsals (e.g., *Avimimus, Adasaurus, Albinykus,*

435   *Elmisaurus*; Kurzanov 1981; Osmólska 1981; Nesbitt et al. 2011; Turner et al. 2012). However,

436   the extensive coossification of the metatarsal shafts is a character present only in *Balaur* and

437   pygostylians (e.g., *Bauxitornis, Confuciusornis, Evgenavis, Hollanda, Patagopteryx, Vorona,*

438   *Yungavolucris*; Chiappe 1993; Chiappe et al. 1999; Chiappe 2002; Forster et al. 2002; Bell et al.

439   2010; Dyke and Ősi 2010; O'Connor et al. 2014; see Fig. 4c, Fig. S3, Fig. S4C-D).

440   *Metatarsals with one or more longitudinal eminences on the dorsal surface of the shafts*

441   The shafts of *Balaur*'s second to fourth metatarsals are dorsoventrally deep in cross-section,

442   being strongly convex along the extensor surfaces except for the area of contact between

443   metatarsals II and III. Here, the lateral edge of metatarsal II and the medial edge of metatarsal III

444   form dorsoventrally shallow, longitudinally arranged flanges that, together, form a depressed

445   region between the remainder of the metatarsal shafts. This unusual character combination,

446   which is not observed in non-avialan theropods, was considered to be an autapomorphy of

447   *Balaur* by Brusatte et al. (2013). However, comparable features are present in several Mesozoic

448   avialans. *Vorona* possesses two distinct ridges that extend along the distal halves of the extensor

449   surfaces of both metatarsals III and IV, delimiting a depressed intermetatarsal space (Forster et

450   al. 2002). A depressed area between metatarsals II and III is also present in *Patagopteryx*

451   (Chiappe 2002). The extensor surfaces of metatarsals II and III are markedly convex transversely

452   in many avisaurids with depressed areas present between the metatarsal shafts (e.g., *Avisaurus,*

453   *Bauxitornis*; Chiappe 1993; Dyke and Ősi 2010; Fig. S3H). *Yungavolucris* is reported to lack a

454   dorsally convex third metatarsal; however, the shaft's extensor surface at the proximal end of

455   metatarsal III bears a centrally positioned, longitudinally oriented eminence comparable to the

456   condition in *Balaur* (Chiappe 1993). Finally, the enigmatic avialan *Mystiornis* also bears distinct

457   longitudinal ridges along the extensor surfaces of metatarsals II-IV (Kurochkin et al. 2010).

458   *Enlarged extensor fossa on distal end of metatarsal II*

459   In most theropods, the distal end of metatarsal II bears an extensor fossa proximal to the articular

460   end. This fossa usually appears as a pit delimited by distinct margins and does not extend

461   mediolaterally across the entire extensor surface (e.g., *Allosaurus, Deinonychus, Tyrannosaurus*;

462   Ostrom 1969; Madsen 1976; Brochu 2003). In *Balaur*, the extensor fossa of metatarsal II is

463   enlarged and extends across the whole distal surface, bounded laterally by a raised ridge

464   converging with the trochlea (Brusatte et al. 2013; Fig. S3B). A large, proximodistally enlarged

465   extensor fossa is present on the second metatarsal of *Evgenavis* (O'Connor et al. 2014; Fig. S3F).

466   An enlarged extensor fossa on metatarsal II, lacking distinct margins and bounded laterally by a

467   raised margin, is also present in *Parabohaiornis* (Wang et al. 2014a) and *Yungavolucris*

468   (Chiappe 1993; Fig. S3E).

469   *Metatarsal II with plantarly projected medial condyle*

470   *Balaur* bears a plantarly projected medial condyle on the distal end of metatarsal II, visible in

471   medial view as a distinct ventral projection of the distal end (Brusatte et al. 2013; Fig. S3A). In

472   most theropods, including dromaeosaurids, the medial condyle of metatarsal II does not project

473   plantarly more than the lateral condyle (e.g., *Deinonychus, Eustreptospondylus, Falcarius,*

474   *Garudimimus, Sinraptor, Talos*, *Tyrannosaurus, Zuolong*; Ostrom 1969; Currie and Zhao 1993;

475   Brochu 2003; Kirkland et al. 2004; Kobayashi and Barsbold 2005; Sadleir et al. 2008; Choiniere

476   et al. 2010; Zanno et al. 2011). Many avialans bear a plantarly unexpanded medial condyle on

477   metatarsal II and hence resemble other theropods (e.g., *Avisaurus, Mystiornis, Yungavolucris*;

478   Chiappe 1993; Kurochkin et al. 2010). However, a plantarly projected medial condyle like that

479   present in *Balaur* is present in the basal pygostylians *Confuciusornis* and *Evgenavis* (O'Connor

480   et al. 2014; Fig. S3G, I) and in the ornithuromorph *Apsaravis* (Clarke and Norell 2002).

481   *Metatarsal II lacks prominent ginglymoid distal end*

482   The presence of a prominent extensor sulcus on the second metatarsal is regarded as a

483   synapomorphy of Dromaeosauridae (Turner et al. 2012). *Balaur* possesses a broadly convex

484   distal end of metatarsal II that lacks a ginglymoid distal articulation with a well-developed

485   extensor sulcus (Fig. 4a; see Norell and Makovicky 1997; Brusatte et al. 2013; Fig. S3B). Some

486   avialan taxa also bear a distinct extensor sulcus on metatarsal II like that present in

487   dromaeosaurids (e.g., *Avisaurus, Yungavolucris*; Chiappe 1993; Fig. S3C, E) whereas others bear

488   a broadly convex articular facet and hence resemble *Balaur* (e.g., *Bauxitornis, Evgenavis*; Dyke

489   and Ősi 2010; O'Connor et al. 2014; Fig. S3D, F).

490   *Distal articular surface of metatarsal II narrower than maximum width of its distal end*

491   The width of the distal articular surface of metatarsal II in *Balaur* is less than the width of the

492   entire distal end of the metatarsal (Brusatte et al. 2013; Fig. S3B). In extensor view, a large non-

493   articular region is present both lateral and medial to the articular surface. The metatarsals of most

494   therizinosauroids show a similar condition (e.g., *Segnosaurus*; Perle 1979). The same feature

495   also occurs in the second metatarsal of some avisaurid avialans, where distinct non-articular

496   mediolateral expansions are present proximal to the distal articular surface (*Avisaurus*

497   *archibaldi*, *A. gloriae*; Chiappe 1993; Varricchio and Chiappe 1995; Fig. S3C).

498   *Shaft of metatarsal IV anteroposteriorly compressed and mediolaterally widened*

499   In most theropods, the mid-length cross section of metatarsal IV is subcircular, or

500   anteroposteriorly thicker than wide. In *Balaur*, the mid-length cross section of metatarsal IV is

501   anteroposteriorly compressed and mediolaterally expanded (Brusatte et al. 2013), a characteristic

502   that is also seen in both velociraptorine (e.g., *Deinonychus*, *Velociraptor* and *Adasaurus*) and

503   dromaeosaurine dromaeosaurids (e.g., *Utahraptor*), as well as basal troodontids (Turner et al.

504   2012). However, an anteroposteriorly compressed metatarsal IV with a flat cross section is also

505   present in basal avialans (e.g., *Avisaurus*, *Mystiornis*, *Evgenavis*, *Yungavolucris*; Brett-Surman

506   and Paul 1985; Chiappe 1993; Kurochkin et al. 2010; O'Connor et al. 2014; Fig. S3E, H).

507   *Short and robust metatarsal V*

508   Dromaeosaurids bear a slender and elongate metatarsal V that is at least 40% of metatarsal III's

509   length (Fig 5c; Norell and Makovicky 1999; Hwang et al. 2002; Brusatte et al. 2013). *Balaur*

510   possesses a shorter and stouter metatarsal V that is less than 30% of metatarsal III's length (Fig

511   5a, Fig. S3A, S4B; Brusatte et al. 2013): it is thus more similar to the condition present in basal

512   avialans (e.g., *Evgenavis, Sapeornis, Vorona*; Forster et al. 2002; Zhou and Zhang 2003;

513   O'Connor et al. 2014) and most non-avialan coelurosaurs (e.g., *Khaan*, *Segnosaurus*,

514   *Tyrannosaurus*; Perle 1979; Brochu 2003; Balanoff and Norell 2012).

515   *Hallux unreduced compared to other toes and functional*

516   *Balaur* possesses a hallux that cannot be considered reduced in size compared to the other pedal

517   digits (Brusatte et al. 2013, Fig. S4B). Most non-avialan theropods, including dromaeosaurids,

518   possess a relatively small first pedal ungual (e.g., *Allosaurus*, *Microraptor*, *Velociraptor*;

519   Madsen 1976; Norell and Makovicky 1997; Hwang et al. 2002; Fig. S4A). However, a large and

520   falciform first pedal ungual that is not reduced compared to the other pedal unguals, as seen in

521   *Balaur*, is also present in many basal avialans (e.g., *Confuciusornis*, *Jixiangornis*, *Patagopteryx*,

522   *Sapeornis*, *Zhouornis*; Chiappe et al. 1999; Chiappe 2002; Ji et al. 2002; Zhou and Zhang 2003;

523   Zhang et al. 2013; Fig. S4D). Furthermore, the first phalanx in *Balaur*'s hallux is subequal in

524   length compared to the proximal phalanges of pedal digits II-IV, a condition present in basal

525   avialans (e.g., *Jixiangornis*, *Sapeornis*, *Zhouornis*; Ji et al. 2002; Zhou and Zhang 2003; Zhang et

526   al. 2013; Fig. S4) but not in non-avialan theropods. The distal placement of the articular end of

527   metatarsal I in *Balaur* relative to the trochlea of metatarsal II is more similar to that of basal

528   avialans (e.g., *Confuciusornis*, *Patagopteryx*; Chiappe et al. 1999; Chiappe 2002) than the more

529   proximally placed trochlea of metatarsal I in dromaeosaurids (e.g., *Microraptor*, *Deinonychus*,

530   *Velociraptor*; Norell and Makovicky 1997; Hwang et al. 2002; Fowler et al. 2011) and other

531   non-avialan theropods (e.g., *Khaan*, Balanoff and Norell 2012). In addition, the well-developed

532   articular surfaces indicate that the hallux of *Balaur* was dextrous, mobile and fully functional

533   (Brusatte et al. 2013). This is also the condition present in birds but contrasts with that of most

534   non-avialan theropods, including dromaeosaurids (Norell and Makovicky 1997).

535   *Enlarged pedal ungual II lacking both marked falciform shape and prominent flexor tubercle*

536   *Balaur* bears a hypertrophied second pedal ungual that is larger than the third and fourth pedal

537   unguals, similar to that seen in most deinonychosaurs (Turner et al. 2012; Brusatte et al. 2013).

538   However, Brusatte et al. (2013) noted that the second pedal ungual of *Balaur* does not show the

539   marked falciform shape and prominent flexor tubercle seen in most dromaeosaurids (e.g.,

540   Ostrom 1969; Turner et al. 2012). A robust second pedal digit with an enlarged and moderately

541   recurved ungual, comparable to the condition in *Balaur*, is also present among several avialans

542   (e.g., *Bohaiornis*, *Fortunguavis*, *Jixiangornis*, *Parabohaiornis*, *Patagopteryx*, *Qiliania*, *Sulcavis*,

543   *Zhouornis*; Chiappe 2002; Ji et al. 2002; Hu et al. 2011; Ji et al. 2011; O'Connor et al. 2013;

544   Zhang et al. 2013; Wang et al. 2014b; Wang et al. 2014A; Fig. S4D).

545   *Penultimate phalanges of pedal digit III more than 1.2 times longer than preceding phalanx*

546   In most theropods, including dromaeosaurids, the penultimate phalanx of the third pedal digit is

547   subequal to or shorter than the length of the preceding phalanges (e.g., *Gallimimus*, *Khaan*,

548   *Tyrannosaurus*, *Velociraptor*; Osmólska et al. 1972; Norell and Makovicky 1997; Brochu 2003;

549   Balanoff and Norell 2012; Brusatte et al. 2013, table 7). However, *Balaur* bears a relatively

550   elongate penultimate phalanx on pedal digit III that is 1.2 times longer than the preceding

551   phalanx (Brusatte et al. 2013; Fig. S4B). This condition is similar to that present in many

552   avialans (e.g., *Concornis*, *Sapeornis*, *Zhouornis*; Sanz et al. 1995; Zhou and Zhang 2003; Zhang

553   et al. 2013; Fig. S4D) and unlike that of dromaeosaurids and most non-avialan theropods.

554   *Pedal ungual IV reduced in size*

555   *Balaur*'s fourth pedal ungual, although distally incomplete in the holotype specimen, is the

556   smallest of the pedal unguals (about 60% the size of pedal ungual III, see Brusatte et al. 2013;

557   Fig. S4B). This condition differs from that seen in dromaeosaurids, *Sapeornis* and some

558   troodontids in which the fourth pedal unguals are more than 85% the length of the third pedal

559   ungual (e.g., *Borogovia* 140%, *Sapeornis* 100%; Osmólska 1987; Brusatte et al. 2013, table 7; Pu

560   et al. 2013). It does, however, resemble the condition in ornithothoracine birds (e.g., *Bohaiornis*

561   59%, *Parabohaiornis* 60%, *Qiliania* 76%, *Zhouornis* 66%; Hu et al. 2011; Ji et al. 2011; Zhang

562   et al. 2013; Fig. S4C-D). The relative length of the fourth pedal ungual in most maniraptorans is

563   intermediate between *Balaur* and dromaeosaurids, being 70-85% the length of pedal ungual III

564   (e.g., *Archaeopteryx* 77-78%, *Khaan*, *Jixiangornis*, *Sinornithoides* and *Zhongjianornis* 80%;

565   Elzanowski 2001; Currie and Dong 2001; Ji et al. 2002; Zhou and Li 2010; Balanoff and Norell

566   2012, fig. 33).

567   **Results**

568   *Modified Brusatte et al. (2014) analysis*

569   The modified Brusatte et al. (2014) analysis produced >999,999 shortest cladograms of 3397

570   steps each (CI = 0.3206, RI = 0.7771). In all the shortest trees found, *Balaur* was recovered as an

571   avialan, as the sister-taxon of *Sapeornis*, and not as a member of Dromaeosauridae. The '*Balaur*

572   *+ Sapeornis'* clade resolved as the sister-taxon of a clade including Pygostylia, *Jixiangornis* and

573   *Jeholornis*. Exploration of the alternative topologies that we recovered resulted in

574   *Epidendrosaurus*, *Hesperonychus*, *Kinnareemimus*, *Pedopenna*, *Pyroraptor*, and *Shanag* acting

575   as 'wildcard' taxa among Maniraptora, and these taxa were pruned *a posteriori* from the results

576   of the analyses to improve resolution within paravian taxa. After pruning the 'wildcard' taxa

577   from the strict consensus topology (Fig. 5), *Archaeopteryx* was resolved as the sister-group to the

578   rest of Avialae. Unambiguous synapomorphies for the sister taxon relationships between *Balaur*

579   and *Sapeornis* are: anterior surface of deltopectoral crest with distinct muscle scar near lateral

580   edge along distal end of crest for insertion of biceps muscle (139.1, homoplastic among

581   maniraptorans); third manual digit with two or less phalanges (147.2, convergently developed

582   among ornithothoracines); humeral condyles placed on anterior surface (366.1, convergently

583   developed among therizinosauroids, alvarezsauroids and most avialans); anteroposterior

584   diameter of metacarpal III less than 50% of the same diameter in metacarpal II (386.1); and

585   length of first phalanx of pedal digit I greater than 66% of first pedal phalanx of pedal digit III

586   (859.1, convergently developed among more crownward avialans).

587   Furthermore, all three versions of the dataset that used implied weighting recovered *Balaur* as an

588   avialan more crownward than *Archaeopteryx* (see Figure S5).

589   *Modified Lee et al. (2014) analysis*

590   The modified Lee et al. (2014) analysis recovered 1152 shortest trees of 6350 steps each (CI =

591   0.2672, RI = 0.5993). The strict consensus of the shortest trees found is in general agreement

592   with the Maximum Clade Credibility Tree recovered by Lee et al. (2014), the most relevant

593   difference being the unresolved polytomy among *Aurornis*, *Jinfengopteryx*, Dromaeosauridae,

594   Troodontidae and Avialae (Fig. 6). The *a posteriori* pruning of the above mentioned genera does

595   not resolve the polytomy among the three suprageneric clades. It is noteworthy that an

596   unresolved polytomy among the main paravian lineages was also obtained by Brusatte et al.

597   (2014), and by our updated version of the latter dataset. In all trees found, *Balaur* was resolved

598   as a basal avialan and as the sister taxon of Pygostylia (the '*Zhongjianornis* + (*Sapeornis* + more

599   crownward avialans)' clade), in agreement with the results of previous versions of this matrix

600   (i.e., Godefroit et al. 2013b). The character states unambiguously supporting this placement for

601   *Balaur* are: (1) presence of fusion between metacarpal II and the distal carpals (char. 311.1);

602   presence of a mediolaterally slender third metacarpal (char. 322.1); absence of the mediodorsal

603   process on the ischium (char. 423.0); presence of an elongate first phalanx of pedal digit I (char.

604   499.0); and presence of a completely fused tibiotarsus (char. 580.1). Nodal support for this

605   placement was low (Decay Index = 1). However, higher nodal support values for nodes along the

606   less crownward part of Avialae support the placement of *Balaur* in this clade. This interpretation

607   is further supported by the implied weighting analyses of the data set: these analyses consistently

608   recovered *Balaur* as a non-pygostylian member of Avialae, located less crownward within

609   Avialae than was the case in the unweighted analysis, and bracketed by *Archaeopteryx* and all

610   other avialans (see Figure S6).

611   *Templeton tests*

612   We re-analysed the original dataset of Brusatte et al.'s (2014) enforcing the following backbone

613   constraint: ((*Balaur*, *Anas*), *Troodon*, *Dromaeosaurus*) (i.e., enforcing the analysis to retain only

614 those topologies where *Balaur* is closer to modern birds than to either troodontids and

615 dromaeosaurids, thus by definition forcing it to be a member of Avialae; see Electronic

616 Supplementary Material). The shortest enforced topologies that resulted were 3368 steps long,

617 eight steps less parsimonious than the shortest unconstrained topologies that recovered *Balaur*

618 among Dromaeosauridae. This difference was not statistically significant based on the

619 Templeton test ($p>0.2059$, N>37).

620 We also re-analysed the modified dataset of Brusatte et al. (2014), this time enforcing *Balaur* to

621 be a dromaeosaurid using the following backbone constraint: ((*Balaur*, *Dromaeosaurus*),

622 *Troodon*, *Anas*). The shortest enforced topologies that resulted were 3400 steps long, three steps

623 less parsimonious than the shortest unconstrained topologies where *Balaur* was recovered within

624 Avialae. This difference was not statistically significant based on the Templeton test ($p>0.7098$,

625 N>61).

626   Using the dataset modified from Lee et al. (2014), we enforced a dromaeosaurid

627 placement for *Balaur*, using the following backbone constraint: ((*Balaur*, *Dromaeosaurus*),

628 *Troodon*, *Meleagris*). The shortest trees found using that constraint are nine steps longer than the

629 shortest unforced topologies, and placed *Balaur* as the basalmost dromaeosaurid, excluded from

630 the ((Eudromaeosauria + Microraptoria) + Unenlagiinae) clade. This difference was not

631 statistically significant based on the Templeton test ($p>0.4400$, N>125).

632   Finally, we also tested a velociraptorine placement for *Balaur*, using the following

633 backbone constraint: ((*Balaur*, *Velociraptor*), *Dromaeosaurus*, *Troodon*). The shortest trees

634 found using that constraint are 14 steps longer than the shortest unforced topologies, and placed

635 *Balaur* as the basalmost velociraptorine. This difference was not statistically significant based on

636 the Templeton test ($p>0.1580$, N>89).

637

638 **Discussion**

639 *Balaur* possesses a unique and bizarre mix of characters, many of which were previously

640 considered exclusive to Deinonychosauria or Avialae, and which may challenge its placement in

641 either of the aforementioned clades. Godefroit et al. (2013b) tested alternative placements of

642 *Balaur* among Paraves, and recovered the dromaeosaurid placement for that taxon as a

643 suboptimal solution. Here, we have shown that an avialan placement for *Balaur* using the

644 original dataset of Brusatte et al. (2014) is a suboptimal solution that cannot be rejected using

645   that dataset. Although the most parsimonious results of the two updated phylogenetic analyses

646   presented here concur in resolving *Balaur* within Avialae, the deinonychosaurian placement for

647   this taxon discussed by Brusatte et al. (2013) can be only tentatively rejected based on current

648   information. The most parsimonious placement was recovered under both equally weighted and

649   implied weighting analyses, suggesting that the avialan placement of *Balaur* was not biased by *a*

650   *priori* assumptions on homoplasious character downweighting. Nevertheless, whatever the

651   placement for *Balaur*, a significant amount of homoplasy, due to both convergences and

652   reversals, is required to explain its unique morphology.

653   The sister taxon relationship recovered between *Balaur* and the short-tailed *Sapeornis* – resulting

654   from analysis of the dataset modified from Brusatte et al. (2014) – is quite unexpected, and may

655   be partially biased by the placement of the long-tailed *Jeholornis* and *Jixiangornis* as closer to

656   other short-tailed birds than *Sapeornis* (a relationship also recovered by the original dataset,

657   Brusatte et al. 2014). According to that topology, the short pygostyle-bearing tail of *Sapeornis*

658   evolved independently of the same condition in more crownward birds. The topology that results

659   from our use of the dataset modified from Lee et al. (2014) agrees with most analyses of avialan

660   relationships (e.g., Cau and Arduini 2008; O'Connor et al. 2011, 2013; Wang et al. 2014b) in

661   depicting a single origin of the pygostylian tail among birds.

662   Here we should note that topological discrepancies and alternative placements of

663   problematic taxa may be influenced by artefacts in coding practice, or by the logical basis of

664   character statement definition followed by different authors (Brazeau 2011). The datasets of

665   Brusatte et al. (2014) and Lee et al. (2014) differ from each other in the logical basis of their

666   respective character statements and definitions. The definitions of many characters used in the

667   analysis of Brusatte et al. (2014) impose congruence by linking more than one variable character

668   to a particular state (see Brazeau 2011 and references therein), or by mixing together neomorphic

669   and transformational characters as alternative states of the same character statements (see Sereno

670   2007). For example, the ordered character 178 of Brusatte et al. (2014) includes three

671   transformational states describing alternative extensions of the pubic apron along the pubis,

672   together with a fourth state describing a distinct phenomenon, the absence of the pubic apron (a

673   neomorphic character). Set that way, the absence of the pubic apron is *a priori* forced as a highly

674   derived (and much weighted) terminal state of a character describing a feature (the proximodistal

675   extent of the apron) that cannot be determined in those taxa lacking the apron. Character

676   statements and definitions in the analysis of Lee et al. (2014) followed the recommendations

677   outlined by Sereno (2007) and Brazeau (2011); consequently, each character statement describes

678   a single variable character, and neomorphic and transformational characters were included as

679   separate character statements. To avoid the creation of spurious transformational optimizations

680   under some topologies, the characters in the analysis of Lee et al. (2014) were therefore atomized

681   in such a way as to capture both the presence or absence of the feature in addition to the states of

682   the feature (Brazeau 2011). Taxa scored as lacking a particular neomorphic character were

683   scored as 'unknown' for the transformational characters describing different conditions of the

684   same neomorphic feature.

685   We therefore consider it likely that some discrepancies between the updated analyses of

686   Brusatte et al. (2014) and Lee et al. (2014) – including the alternative placements of *Balaur* and

687   *Sapeornis* among basal avialans – reflect artefacts of coding rather than actual conflict in the

688   data. Nevertheless, it is noteworthy that even using distinct datasets, alternative character

689   weighting hypotheses and different logical bases for character definitions, *Balaur* was

690   consistently recovered as a basal avialan. Furthermore, the phylogenetic analysis of Foth et al.

691   (2014), which used the dataset of Turner et al. (2012) as their basis and which included an

692   expanded set of characters, independently found *Balaur* to be a basal avialan more crownward

693   than *Archaeopteryx*, but in a less crownward position than that presented here. In conclusion, we

694   consider the consensus among the results of these alternative tests (i.e., *Balaur* as a non-

695   pygostylian basal avialan) as the phylogenetic framework for the discussion on its evolution and

696   palaeoecology.

697   *Implications for the palaeoecology of* Balaur

698   In the absence of both extrinsic data on diet and craniodental remains there is no direct evidence

699   pertaining to the ecology and trophic adaptations of *Balaur*. Although not explicitly stated,

700   Brusatte et al.'s (2013) inferences regarding the ecology and diet of *Balaur* rest entirely on their

701   favoured phylogenetic placement of the taxon within the predatory deinonychosaurian clade

702   Velociraptorinae (see Carpenter 1998).

703   However, some aspects of *Balaur*'s morphology do not support the hypothesis that its

704   ecomorphology was similar to that of dromaeosaurids. While there exists evidence that

705   dromaeosaurids employed both their hands and feet in predation (see Carpenter 1998), the

706   reduction in length and functionality of the third manual digit and the poor development or

707   absence of the pedal characters linked with predatory behaviour in deinonychosaurs (i.e.,

708   ginglymoid distal end of metatarsal II allowing extensive hyperextension, falciform second

709   ungual with prominent flexor tubercle; Ostrom 1969; Fowler et al. 2011), challenge the notion of

710   a specialised, dromaeosaurid-like predatory ecology for *Balaur*. Brusatte et al. (2013) interpreted

711   these unusual traits of *Balaur* as the result of insularism, although they acknowledged that

712   comparable morphological changes in insular taxa have so far not been reported in predatory

713   species. We are not aware of the reduction or loss of predatory adaptations in any insular

714   predatory taxon, and therefore consider it unlikely that the unique morphology of *Balaur*, in

715   particular the appendicular characters considered to be predatory adaptations among

716   dromaeosaurids, could be sufficiently accounted for by the 'island effect'.

717   Most of the features considered to be autapomorphies of *Balaur* by Csiki et al. (2010) and

718   Brusatte et al. (2013) are reinterpreted here as avialan synapomorphies. Consequently, these

719   traits were inherited by *Balaur* from its bird-like ancestors before its lineage was isolated in the

720   Hațeg environment. Since our analyses place *Balaur* among a grade of non-predatory avialans

721   including herbivorous and/or omnivorous species (Zhou and Zhang 2002; Dalsätt et al. 2006;

722   Zanno and Makovicky 2011), our preferred scenario does not necessitate a hypothesis of a

723   carnivorous ecology for this taxon and is thus more consistent with the absence of the

724   aforementioned predatory adaptations. Furthermore, in assuming a herbivorous or omnivorous

725   ecology for *Balaur*, the amount of morphological changes, particularly in limb shapes and

726   proportions, is comparable to that reported in several insular herbivorous and omnivorous taxa,

727   including both mammals (Sondaar 1977; Caloi and Palombo 1994; van der Geer et al. 2011) and

728   dinosaurs (e.g., Dalla Vecchia 2009). In particular, the presence in *Balaur* of a relatively broad

729   pelvic canal, the short and broad metatarsus with mediolaterally expanded distal ends relative to

730   the articular surfaces, and the presence of an enlarged first pedal digit is a combination of

731   features convergently acquired only by the non-predatory clade Therizinosauridae among

732   Mesozoic theropods (Zanno 2010; Zanno and Makovicky 2011).

733   However, we agree with previous authors that, regardless of its position within Paraves,

734   the morphology of *Balaur* includes a unique and unexpected combination of features, otherwise

735   seen in distinct maniraptoran lineages. Interestingly, *Balaur* independently evolved a series of

736   features previously reported in more crownward bird lineages, such as a deep *depressio*

737   *epicondylaris medialis* in the tibiotarsus, a hypertrophied extensor fossa in the second metatarsal,

738 and dorsally convex metatarsals with expanded distal ends (characters elsewhere seen in some

739 ornithothoracines). A possible role of insularism in the origin of some of these traits is

740 acknowledged even in our preferred phylogenetic scenario. In particular, the results of our

741 analyses indicate that *Balaur* is phylogenetically bracketed by taxa showing relatively more

742 elongate forelimbs (humeral lengths usually more than 60% of the tibiotarsus + tarsometatarsus

743 length) and more robust forearms (ulna as thick as or thicker than the tibiotarsus). Accordingly,

744 we interpret the forelimb of *Balaur* as secondarily reduced. Flightlessness has also been inferred

745 in the ornithurine *Gargantuavis* from the Campanian-Maastrichtian of southern France

746 (Buffetaut and Loeuff 1998), indicating that distinct avialan lineages endemic to Late Cretaceous

747 Europe reduced or lost their flight adaptations. Several bird clades independently evolved

748 flightlessness during the Cenozoic as a result of their exploitation of insular environments and

749 the taxa concerned typically displayed apomorphic reduction of the forelimbs compared to those

750 of their closest relatives (Paul 2002; Naish 2012). Therefore, the reduced forelimb of *Balaur* may

751 be interpreted as the result of insularism.

752   Finally, existing skeletal and life reconstructions of *Balaur* have interpreted it as a

753 velociraptorine-like dromaeosaurid (Csiki et al. 2010; Brusatte et al. 2013). Does our re-

754 interpretation of this taxon as a member of Avialae require that previous hypotheses about its

755 appearance should be modified? By combining the known elements of *Balaur* with those of other

756 paravians, a new skeletal reconstruction has been produced (Fig. 7). As our knowledge of

757 Mesozoic paravian diversity has improved, it has become ever clearer that early members of the

758 deinonychosaurian and avialan lineages were highly similar in proportions, detailed anatomy and

759 life appearance: consequently, an 'avialan interpretation' of *Balaur* does not result in an animal

760 obviously different from a 'dromaeosaurid interpretation'. This conclusion has been supported

761 by recent quantitative analyses that demonstrate a significant degree of shared morphospace

762 between basal avialan taxa and their closest paravian relatives (e.g., Brusatte et al. 2014).

763 Nevertheless, we suggest that *Balaur* may have been proportionally shorter-tailed and with a less

764 raptorial-looking foot than previously depicted (Csiki et al. 2010; Brusatte et al. 2013). Clearly,

765 details of its cranial and dental anatomy are speculative. We assume that, like other paravians,

766 *Balaur* was extensively feathered.

767 **Conclusions**

768 The Maastrichtian paravian theropod *Balaur bondoc* is reinterpreted here as a basal avialan

769   rather than as a dromaeosaurid. Features supporting its placement among Avialae include the

770   hypertrophied and proximally placed coracoid tubercle, the anterior placement of the condyles of

771   the humerus, the proximally fused carpometacarpus with a laterally shifted semilunate carpal, the

772   closed intermetacarpal space, the reduced condyles on metacarpals I-II, the slender metacarpal

773   III, the reduced phalangeal formula of the third digit, the extensively fused tibiotarsus, the

774   extensively fused tarsometatarsus, the distal placement of the articular end of first metatarsal, the

775   large size of the hallux, and the elongation of the penultimate phalanges of the pes. The absence

776   of dromaeosaurid synapomorphies (e.g., non-ginglymoid metatarsals II and III, short metatarsal

777   V) is thus interpreted as plesiomorphic, and not as the consequence of evolutionary reversal.

778   Both its phylogenetic bracketing within basal avialans and the absence of predatory adaptations

779   concur in indicating that *Balaur* was herbivorous or omnivorous, not predatory. The reduced

780   forelimb of *Balaur* represents one of the most compelling pieces of evidence for insular

781   adaptation in a Mesozoic bird. Furthermore, with its unique combination of features shared by

782   distinct paravian clades and its possible placement as one of the closest relatives of Pygostylia,

783   *Balaur* may represent a pivotal taxon in future investigations of Mesozoic bird interrelationships.

784   The hypothesis that some Mesozoic paravians represent the flightless descendants of

785   volant, *Archaeopteryx*-like ancestors, most vigorously promoted by Paul (1988, 2002), has not

786   been supported by recent phylogenetic hypotheses (e.g., Senter 2007b; Turner et al. 2012;

787   Agnolín and Novas 2013). Furthemore, phylogenetic analyses that incorporate sufficient

788   character data are able to differentiate the members of such paravian lineages as

789   Dromaeosauridae, Troodontidae and Avialae, as demonstrated by our present study.

790   Nevertheless, reinterpretation of *Balaur* as a flightless avialan reinforces the point that at least

791   some Mesozoic paravian taxa, highly similar in general form and appearance to dromaeosaurids,

792   may indeed be the enlarged, terrestrialised descendants of smaller, flighted ancestors, and that

793   the evolutionary transition involved may have required relatively little in the way of

794   morphological or trophic transformation.

795   **Acknowlegements**

796   We thank staff at the Transylvanian Museum Society (EME), Cluj-Napoca, in particular Matyas

797   and Marta Vremir for allowing access to the *Balaur* holotype, for discussion and substantial

798   invaluable assistance in Transylvania. DN and TB's work in Romania was funded by the

799   National Geographic Society. Critical comments by James Clark, Michael Pittman, and

800   Academic Editor John Hutchinson greatly improved the quality of the manuscript. We thank

801   Steve Brusatte, Jonah Choiniere, Gareth Dyke and Corwin Sullivan for the detailed and critical

802   comments on an earlier version of this manuscript. The program TNT is being made available

803   with the sponsorship of the Willi Hennig Society. Jaime Headden kindly created and allowed use

804   of the image in Fig. 7.

805

806   **Figure captions**

807   Figure 1. Comparison of the scapulocoracoid of (A) *Balaur* (lateral view) to that of (B) the

808   pygostylian *Enantiophoenix* (medial view); and (C) the dromaeosaurid *Velociraptor* (lateral

809   view); (A) after Csiki et al. (2010, fig. 1); (B) modified after Cau and Arduini (2003, fig. 2); (C)

810   after Norell and Makovicky (1999, fig. 4). All scapulocoracoids are drawn with the proximal half

811   of the scapular blade oriented horizontally to show relative placement of coracoid tubercle. Scale

812   bar: 10 mm (A); 5 mm (B); 10 mm (C). Abbreviations: ac, acromion; co, coracoid; ct, coracoid

813   tubercle; gl, glenoid; me, missing element; sc, scapula; snf, supracoracoid nerve foramen.

814   Figure 2. Comparison of the manus of (A) *Balaur* to those of (B) the enantiornithine *Zhouornis*;

815   (C) the pygostylian *Sapeornis*; and (D) the dromaeosaurid *Deinonychus*, showing bird-like

816   features of *Balaur*. (A) after Csiki et al. (2010, fig. 1, mirrored from original); (B) after Zhang et

817   al. (2013, fig. 7); (C) after Zhou and Zhang (2003, fig. 7); (D) after Wagner and Gauthier (1999,

818   fig. 2). All drawn at the same metacarpal II length. Scale bar: 20 mm (A, D); 10 mm (B, C).

819   Abbreviations: cis, closed intermetacarpal space; cmc, carpometacarpus; d3, reduced third digit;

820   drc, distally restricted condyles; lsc, laterally shifted semilunate carpal; p1-III, first phalanx of

821   manual digit 3; p2-III, second phalanx of manual digit 3; pec, proximally expanded extensor

822   surface; pnm, proximally narrow metacarpal I; U, ungual; usc, unfused semilunate carpal.

823   Figure 3. Pelvis of *Balaur* in lateral view (A). Comparison of the pubes of *Balaur* in

824   anteroventral view (B) to those of the pygostylian *Sapeornis* in anterior view (C), and the

825   dromaeosaurid *Velociraptor* in posterior view (D). (C) after Zhou and Zhang (2003, fig. 8); (D)

826   after Norell and Makovicky (1999, fig. 19). Scale bar: 10 mm (A, B, D), 2 mm (C).

827   Abbreviations: aa, antitrochanter; ac, acetabulum; cf, cuppedicus fossa; dfi, dorsal flange of

828   ischium; ipf, interpubic fenestra; is, ischium; pa, pubic apron; ps, pubic symphysis; pu, pubis,

829   sv, sacral vertebrae.

830   Figure 4. Comparison of the metatarsus and pes of (B) *Balaur* to that of (A) the dromaeosaurid

831   *Velociraptor*; and (C) the pygostylian *Zhouornis*. (A) after Norell and Makovicky (1997 figs. 6);

832   (C) after Zhang et al. (2013, fig. 8, mirrored from original). Scale bar: 20 mm (A, B); 10 mm (C).

833   Abbreviations: mt I, metatarsal I; mt V, metatarsal V; tt, tibiotarsus; U II: pedal ungual II; U IV,

834   pedal ungual IV.

835   Figure 5. Reduced strict consensus of the shortest trees from the analysis of the modified

836   Brusatte et al. (2014) matrix after pruning the 'wildcard' taxa *Epidendrosaurus*, *Hesperonychus*,

837 *Kinnareemimus*, *Pedopenna*, *Pyroraptor*, and *Shanag*. Numbers adjacent to nodes indicate

838 Decay Index values >1.

839 Figure 6. Strict consensus tree of the shortest trees from the analysis of the modified Lee et al.

840 (2014) matrix. Numbers adjacent to nodes indicate Decay Index values.

841 Figure 7. Speculative skeletal reconstruction for *Balaur bondoc*, showing known elements in

842 white and unknown elements in grey. Note that the integument would presumably have

843 substantially altered the outline of the animal in life. Produced by Jaime Headden, used with

844 permission.

845

References

846

847 Agnolín FL, Novas FE (2013) Avian Ancestors: A Review of the Phylogenetic Relationships of

848   the Theropods Unenlagiidae, *Microraptor*ia, *Anchiornis* and Scansoriopterygidae. Springer

849 Agnolín FL, Novas FE (2011) Unenlagiid theropods: are they members of the Dromaeosauridae

850   (Theropoda, Maniraptora)? Anais da Academia Brasileira de Ciências 83:117–162.

851 Allain R, Tykoski R, Aquesbi N, Jalil N-E, Monbaron M, Russell D, Taquet P (2007) An

852   abelisauroid (Dinosauria: Theropoda) from the Early Jurassic of the High Atlas Mountains,

853   Morocco, and the radiation of ceratosaurs. Journal of Vertebrate Paleontology 27:610–624.

854 Baier DB, Gatesy SM, Jenkins FA (2007) A critical ligamentous mechanism in the evolution of

855   avian flight. Nature 445:307–310.

856 Balanoff AM, Norell MA (2012) Osteology of *Khaan mckennai* (Oviraptorosauria: Theropoda).

857   Bulletin of the American Museum of Natural History 372:1–77.

858 Barsbold R, Currie PJ, Myhrvold NP, Osmólska H, Tsogtbaatar K, Watabe M (2000) A

859   pygostyle from a non-avian theropod. Nature 403:155–156.

860 Baumel JJ, Witmer LM (1993) Osteologia. In: Baumel JJ, King AS, Breazile JE, Evans HE,

861   Vanden Berge JC (eds) Handbook of avian anatomy: Nomina anatomica avium.

862   Publications of the Nuttall Ornithological Club, no. 25, pp 45–132

863 Bell AK, Chiappe LM, Erickson GM, Suzuki S, Watabe M, Barsbold R, Tsogtbaatar K (2010)

864   Description and ecologic analysis of *Hollanda luceria*, a Late Cretaceous bird from the

865   Gobi Desert (Mongolia). Cretaceous Research 31:16–26.

866 Brazeau MD (2011) Problematic character coding methods in morphology and their effects.

867   Biological Journal of the Linnean Society 104:489–498.

868 Brett-Surman MK, Paul GS (1985) A new family of bird-like dinosaurs linking Laurasia and

869   Gondwanaland. Journal of Vertebrate Paleontology 5:133–138.

870 Brochu CA (2003) Osteology of *Tyrannosaurus rex*: Insights from a nearly complete Skeleton

871   and High-Resolution Computed Tomographic Analysis of the Skull. Journal of Vertebrate

872   Paleontology 22:1–138.

873 Brusatte S, Lloyd G, Wang S, Norell M (2014) Gradual Assembly of Avian Body Plan

874   Culminated in Rapid Rates of Evolution across the Dinosaur-Bird Transition. Current

875   Biology 24:2386–2392.

876 Brusatte SL, Vremir M, Csiki-Sava Z, Turner AH, Watanabe A, Erickson GM, Norell MA

877   (2013) The Osteology of *Balaur bondoc*, an Island-Dwelling Dromaeosaurid (Dinosauria:

878   Theropoda) from the Late Cretaceous of Romania. Bulletin of the American Museum of

879   Natural History 374:1–100.

880 Buffetaut E, Loeuff JL (1998) A new giant ground bird from the Upper Cretaceous of southern

881   France. Journal of the Geological Society 155:1–4.

882 Burnham DA (2004) New information on *Bambiraptor feinbergi* from the Late Cretaceous of

883   Montana. In: Currie PJ, Koppelhus EB, Shugar MA, Wright JL (eds) Feathered Dragons:

884   Studies on the Transition from Dinosaurs to Birds. Indiana University Press, pp 67–111

885 Caloi L, Palombo MR (1994) Functional aspects and ecological implications in Pleistocene

886   endemic herbivores of Mediterranean Islands. Historical Biology 8:151–172.

887 Cau A., Arduini P (2008) *Enantiophoenix electrophyla* gen. et sp. nov. (Aves, Enantiornithes)

888   from the Upper Cretaceous (Cenomanian) of Lebanon and its phylogenetic relationships.

889   Atti della Società Italiana di Scienze Naturali e del Museo Civico di Storia Naturale di

890   Milano 149(II):293–324.

891 Cau A, Dyke GJ, Lee MSY, Naish D (2014) Data from: Sustained miniaturization and

892   anatomical innovation in the dinosaurian ancestors of birds. Dryad Digital Repository doi:

893   http://dx.doi.org/10.5061/dryad.jm6pj

894 Carpenter K (1998) Evidence of predatory behavior by carnivorous dinosaurs. Gaia 15:135–144.

895 Chiappe LM (2002) Osteology of the flightless *Patagopteryx deferrariisi* from the Late

896   Cretaceous of Patagonia (Argentina). In: Chiappe LM, Witmer LM (eds) Mesozoic Birds:

897   above the heads of dinosaurs. University of California Press, pp 281–361

898 Chiappe LM (1993) Enantiornithine (Aves) tarsometatarsi from the Cretaceous Lecho Formation

899   of northwestern Argentina. American Museum Novitates 3083:1–27.

900 Chiappe LM, Shu-an J, Qiang J, Norell MA (1999) Anatomy and Systematics of the

901   Confuciusornithidae (Theropoda Aves) from the Late Mesozoic of Northeast. Bulletin of

902   the American Museum of Natural History 242:1–89.

903 Chiappe LM, Walker CA (2002) Skeletal morphology and systematics of the Cretaceous

904   Euenantiornithes (Ornithothoraces: Enantiornithes). In: Chiappe LM, Witmer LM (eds)

905   Mesozoic Birds: above the heads of dinosaurs. University of California Press, pp 240–267

906 Choiniere JN, Xu X, Clark JM, Forster CA, Guo Y, Han F (2010) A Basal Alvarezsauroid

907   Theropod from the Early Late Jurassic of Xinjiang, China. Science 327:571–574.

908   Clarke JA, Chiappe LM (2001) A new carinate bird from the Late Cretaceous of Patagonia
909   (Argentina). American Museum Novitates 1–24.

910   Clarke JA, Norell MA (2002) The morphology and phylogenetic position of *Apsaravis ukhaana*
911   from the Late Cretaceous of Mongolia. American Museum Novitates 1–46.

912   Csiki Z, Vremir M, Brusatte SL, Norell MA (2010) An aberrant island-dwelling theropod
913   dinosaur from the Late Cretaceous of Romania. Proceedings of the National Academy of
914   Sciences 107:15357–15361.

915   Currie PJ, Paulina Carabajal A (2012) A new specimen of *Austroraptor cabazai* Novas, Pol,
916   Canale, Porfiri and Calvo, 2008 (Dinosauria, Theropoda, Unenlagiidae) from the latest
917   Cretaceous (Maastrichtian) of Río Negro, Argentina. Ameghiniana 49:662–667.

918   Currie PJ, Zhao X-J (1993) A new carnosaur (Dinosauria, Theropoda) from the Jurassic of
919   Xinjiang, People's Republic of China. Can J Earth Sci 30:2037–2081.

920   Currie PJ, Zhiming D (2001) New information on Cretaceous troodontids (Dinosauria,
921   Theropoda) from the People's Republic of China. Can J Earth Sci 38:1753–1766.

922   Dalla Vecchia FM (2009) *Tethyshadros insularis*, a new hadrosauroid dinosaur (Ornithischia)
923   from the Upper Cretaceous of Italy. Journal of Vertebrate Paleontology 29:1100–1116.

924   Dalsätt J, Zhou Z, Zhang F, Ericson PGP (2006) Food remains in *Confuciusornis sanctus* suggest
925   a fish diet. Naturwissenschaften 93:444–446.

926   Dyke GJ, Ősi A (2010) A review of Late Cretaceous fossil birds from Hungary. Geol J 45:434–
927   444.

928   Elzanowski A (2001) A new genus and species for the largest specimen of *Archaeopteryx*. Acta
929   Palaeontologica Polonica 46:519–532.

930   Elzanowski A, Chiappe LM, Witmer LM (2002) Archaeopterygidae (Upper Jurassic of
931   Germany). In: Mesozoic Birds: Above the Heads of Dinosaurs. University of California
932   Press, pp 129–159

933   Forster CA (1998) The Theropod Ancestry of Birds: New Evidence from the Late Cretaceous of
934   Madagascar. Science 279:1915–1919.

935   Forster CA, Chiappe LM, Krause DW, Sampson SD (2002) *Vorona berivotrensis*, a primitive
936   bird from the Late Cretaceous of Madagascar. In: Chiappe LM, Witmer LM (eds)
937   Mesozoic Birds: above the heads of dinosaurs. University of California Press, pp 268–280

938   Foth C, Tischlinger H, Rauhut OWM (2014) New specimen of *Archaeopteryx* provides insights

939   into the evolution of pennaceous feathers. Nature 511:79–82.

940 Fowler DW, Freedman EA, Scannella JB, Kambic RE (2011) The Predatory Ecology of

941   *Deinonychus* and the Origin of Flapping in Birds. PLoS ONE 6:e28964.

942 Gao C, Chiappe LM, Zhang F, Pomeroy DL, Shen C, Chinsamy A, Walsh MO (2012) A

943   subadult specimen of the Early Cretaceous bird *Sapeornis chaoyangensis* and a taxonomic

944   reassessment of sapeornithids. Journal of Vertebrate Paleontology 32:1103–1112.

945 Godefroit P, Cau A, Dong-Yu H, Escuillié F, Wenhao W, Dyke G (2013a) A Jurassic avialan

946   dinosaur from China resolves the early phylogenetic history of birds. Nature 498:359–362.

947 Godefroit P, Demuynck H, Dyke G, Hu D, Escuillié F, Claeys P (2013b) Reduced plumage and

948   flight ability of a new Jurassic paravian theropod from China. Nature Communications

949   4:1394.

950 Goloboff PA (1993) Estimating character weights during tree search. Cladistics 9:83–91.

951 Goloboff PA, Carpenter JM, Arias JS, Esquivel DRM (2008a) Weighting against homoplasy

952   improves phylogenetic analysis of morphological data sets. Cladistics 24:758–773.

953 Goloboff PA, Farris JS, Nixon KC (2008b) TNT, a free program for phylogenetic analysis.

954   Cladistics 24:774–786.

955 Harris J (2004) Confusing dinosaurs with mammals: Tetrapod phylogenetics and anatomical

956   terminology in the world of homology. The Anatomical Record 281A:1240–1246.

957 Harrison CJO, Walker CA (1975) The Bradycnemidae, a new family of owls from the Upper

958   Cretaceous of Romania. Palaeontology 18:563–570.

959 Holtz TR, Jr. (1995) The arctometatarsalian pes, an unusual structure of the metatarsus of

960   Cretaceous Theropoda (Dinosauria: Saurischia). Journal of Paleontology 14: 480–519.

961 Hu D, Li L, Hou L, Xu X (2011) A new enantiornithine bird from the Lower Cretaceous of

962   western Liaoning, China. Journal of Vertebrate Paleontology 31:154–161.

963 Hu D, Xu X, Hou L, Sullivan C (2012) A new enantiornithine bird from the Lower Cretaceous of

964   Western Liaoning, China, and its implications for early avian evolution. Journal of

965   Vertebrate Paleontology 32:639–645.

966 Hutchinson JR (2001) The evolution of pelvic osteology and soft tissues on the line to extant

967   birds (Neornithes). Zoological Journal of the Linnean Society 131:123–168.

968 Hwang SH, Norell MA, Qiang J, Keqin G (2002) New specimens of *Microraptor zhaoianus*

969   (Theropoda: Dromaeosauridae) from northeastern China. American Museum Novitates 1–

970   44.

971   Ji Q, Ji S-A, Zhang H, You H, Zhang J, Wang L, Yuan C, Ji Z (2002) A new avialian bird -
972   *Jixiangornis orientalis* gen. et sp. nov. - from the Lower Cretaceous of Western Liaoning,
973   NE China. Journal of Nanjing University (Natural Science) 38:723–736.

974   Ji S-A, Atterholt J, O'Connor JK, Lamanna MC, Harris JD, Li D-Q, You H-L, Dodson P (2011)
975   A new, three-dimensionally preserved enantiornithine bird (Aves: Ornithothoraces) from
976   Gansu Province, north-western China. Zoological Journal of the Linnean Society 162:201–
977   219.

978   Kirkland JI, Zanno LE, Sampson SD, Clark JM, DeBlieux DD (2004) A primitive
979   therizinosauroid dinosaur from the Early Cretaceous of Utah. Nature 435:84–87.

980   Kobayashi Y, Barsbold R (2005) Reexamination of a primitive ornithomimosaur, *Garudimimus*
981   *brevipes* Barsbold, 1981 (Dinosauria: Theropoda), from the Late Cretaceous of Mongolia.
982   Can J Earth Sci 42:1501–1521.

983   Kurochkin EN, Dyke GJ, Karhu AA (2002) A new presbyornithid bird (Aves, Anseriformes)
984   from the Late Cretaceous of southern Mongolia. American Museum Novitates 1–11.

985   Kurochkin EN, Zelenkov NV, Averianov AO, Leshchinskiy SV (2010) A new taxon of birds
986   (Aves) from the Early Cretaceous of Western Siberia, Russia. Journal of Systematic
987   Palaeontology 9:109–117.

988   Kurzanov SM (1981) On the unusual theropods from the Upper Cretaceous of Mongolia. Trudy
989   Sovmestnay Sovetsko-Mongolskay Paleontologiyeskay Ekspeditsiy (Joint Soviet-
990   Mongolian Paleontological Expedition) 39–49.

991   Lee MSY, Cau A, Naish D, Dyke GJ (2014) Sustained miniaturization and anatomical
992   innovation in the dinosaurian ancestors of birds. Science 345(6196): 562–566.

993   Li L, Ye D, Dongyu H, Li W, Shaoli C, Lianhai H (2006) New eoenantiornithid bird from the
994   Early Cretaceous Jiufotang Formation of Western Liaoning, China. Acta Geologica Sinica
995   - English Edition 80:38–41.

996   Lipkin C, Carpenter K (2008) Looking again at the forelimb of *Tyrannosaurus rex*. In: Larson
997   PL, Carpenter K (eds) *Tyrannosaurus rex*, the Tyrant King. Indiana University Press, pp
998   166–190

999   Longrich NR, Currie PJ (2009) *Albertonykus borealis*, a new alvarezsaur (Dinosauria:
1000   Theropoda) from the Early Maastrichtian of Alberta, Canada: implications for the

1001   systematics and ecology of the Alvarezsauridae. Cretaceous Research 30:239–252.

1002 Madsen JH (1976) *Allosaurus fragilis*: a revised osteology. Utah Geological Survey Bulletin,

1003   Salt Lake City

1004 Makovicky PJ, Apesteguía S, Agnolín FL (2005) The earliest dromaeosaurid theropod from

1005   South America. Nature 437:1007–1011.

1006 Naish D (2012) Birds. In: Brett-Surman MK, Holtz TR, Farlow JO (eds) The Complete Dinosaur

1007   (Second Edition). Indiana University Press, pp 379–423

1008 Nesbitt SJ, Clarke JA, Turner AH, Norell MA (2011) A small alvarezsaurid from the eastern

1009   Gobi Desert offers insight into evolutionary patterns in the Alvarezsauroidea. Journal of

1010   Vertebrate Paleontology 31:144–153.

1011 Norell M, Clark JM, Makovicky PJ (2001) Phylogenetic relationships among coelurosaurian

1012   dinosaurs. In: Ostrom JH, Gauthier J, Gall LF (eds) New perspectives on the origin and

1013   early evolution of birds: proceedings of the International Symposium in honor of John H.

1014   Ostrom. Peabody Museum of Natural History Yale University, pp 49–67

1015 Norell MA, Makovicky PJ (1997) Important Features of the Dromaeosaurid Skeleton

1016   Information from a new specimen. American Museum Novitates 3215:1–28.

1017 Norell MA, Makovicky PJ (1999) Important Features of the Dromaeosaurid Skeleton II:

1018   Information from Newly Collected Specimens of *Velociraptor mongoliensis*. American

1019   Museum Novitates 3282:1–45.

1020 Novas FE (1997) Anatomy of *Patagonykus puertai* (Theropoda, Avialae, Alvarezsauridae), from

1021   the Late Cretaceous of Patagonia. Journal of Vertebrate Paleontology 17:137–166.

1022 Novas FE (2004) Avian traits in the ilium of *Unenlagia comahuensis* (Maniraptora, Avialae). In:

1023   Currie PJ, Koppelhus EB, Shugar MA, Wright JL (eds) Feathered Dragons: Studies on the

1024   Transition from Dinosaurs to Birds. Indiana University Press, pp 137–166

1025 Novas FE, Puerta PF (1997) New evidence concerning avian origins from the Late Cretaceous of

1026   Patagonia. Nature 387:390–392.

1027 O'Connor J, Chiappe LM, Bell AK (2011) Pre-modern birds: avian divergences in the Mesozoic.

1028   In: Dyke DG, Kaiser G (eds) Living Dinosaurs: The Evolutionary History of Modern

1029   Birds. John Wiley & Sons, pp 39–114

1030 O'Connor J, Zhang Y, Chiappe LM, Meng Q, Quanguo L, Di L (2013) A new enantiornithine

1031   from the Yixian Formation with the first recognized avian enamel specialization. Journal of

1032   Vertebrate Paleontology 33:1–12.

1033   O'Connor JK, Averianov AO, Zelenkov NV (2014) A confuciusornithiform (Aves, Pygostylia)-

1034   like tarsometatarsus from the Early Cretaceous of Siberia and a discussion of the evolution

1035   of avian hind limb musculature. Journal of Vertebrate Paleontology 34:647–656.

1036   Osmólska H (1981) Coossified tarsometatarsi in theropod dinosaurs and their bearing on the

1037   problem of bird origins. Palaeontologia Polonica 42:79–95.

1038   Osmólska H (1987) *Borogovia gracilicrus* gen. et sp. n., a new troodontid dinosaur from the Late

1039   Cretaceous of Mongolia. Acta Palaeontologica Polonica 32:133–150.

1040   Osmólska H, Roniewicz E (1970) Deinocheiridae, a new family of theropod dinosaurs.

1041   Palaeontologia Polonica 21:5–19.

1042   Osmólska H, Roniewicz E, Barsbold R (1972) A new dinosaur, *Gallimimus bullatus* n. gen., n.

1043   sp. (Ornithomimidae) from the Upper Cretaceous of Mongolia. Palaeontologia Polonica

1044   27:104–143.

1045   Ostrom JH (1976) *Archaeopteryx* and the origin of birds. Biological Journal of the Linnean

1046   Society 8:91–1982.

1047   Ostrom JH (1969) Osteology of *Deinonychus antirrhopus*, an Unusual Theropod from the Lower

1048   Cretaceous of Montana. Peabody Museul Bulletin 30:1–165.

1049   Paul GS (2002) Dinosaurs of the air: the evolution and loss of flight in dinosaurs and birds. Johns

1050   Hopkins University Press, Baltimore

1051   Paul GS (1988) Predatory dinosaurs of the world: a complete illustrated guide. Simon &

1052   Schuster, New York

1053   Perle A (1979) Segnosauridae - a new family of Theropoda from the Lower Cretaceous of

1054   Mongolia. Trudy, Sovmestnaâ Sovetsko - Mongol'skaâ paleontologičeskaâ èkspediciâ

1055   8:45–55.

1056   Perle A, Chiappe LM, Barsbold R, Clark JM, Norell MA (1994) Skeletal Morphology of

1057   *Mononykus olecranus* (Theropoda Avialae) from the Late Cretaceous of Mongolia.

1058   American Museum Novitates 3105:1–29.

1059   Perle A, Norell MA, Chiappe LM, Clark JM (1993) Flightless bird from the Cretaceous of

1060   Mongolia. Nature 362:623–626.

1061   Perle A, Norell MA, Clark JM (1999) A new maniraptoran theropod, *Achillobator giganticus*

1062   (Dromaeosauridae), from the Upper Cretaceous of Burkhant, Mongolia. Contributions

1063   from the Geology and Mineralogy Chair, National University of Mongolia 1–105.

1064   Pu H, Chang H, Lü J, Wu Y, Xu L, Zhang J, Jia S (2013) A New Juvenile Specimen of

1065   *Sapeornis* (Pygostylia: Aves) from the Lower Cretaceous of Northeast China and

1066   Allometric Scaling of this Basal Bird. Paleontological Research 17:27–38.

1067   Sadleir R, Barrett PM, Powell HP (2008) The anatomy and systematics of *Eustreptospondylus*

1068   *oxoniensis*, a theropod dinosaur from the Middle Jurassic of Oxfordshire, England.

1069   Monograph of the Palaeontographical Society, London

1070   Sanz JL, Chiappe LM, Buscalioni AD (1995) The osteology of *Concornis lacustris* (Aves,

1071   Enantiornithes) from the Lower Cretaceous of Spain and a reexamination of its

1072   phylogenetic relationships. American Museum Novitates 3133:

1073   Senter P (2007a) A method for distinguishing dromaeosaurid manual unguals from pedal "sickle

1074   claws". Bulletin of Gunma Museum of Natural History 11:1–6.

1075   Senter P (2007b) A new look at the phylogeny of coelurosauria (Dinosauria: Theropoda). Journal

1076   of Systematic Palaeontology 5:429–463.

1077   Senter P, Kirkland JI, DeBlieux DD, Madsen S, Toth N (2012) New Dromaeosaurids

1078   (Dinosauria: Theropoda) from the Lower Cretaceous of Utah, and the Evolution of the

1079   Dromaeosaurid Tail. PLoS ONE 7:e36790.

1080   Senter P, Robins JH (2005) Range of motion in the forelimb of the theropod dinosaur

1081   *Acrocanthosaurus atokensis*, and implications for predatory behaviour. Journal of Zoology

1082   266:307–318.

1083   Sereno PC (2007) Logical basis for morphological characters in phylogenetics. Cladistics

1084   23:565–587.

1085   Sereno PC, Chenggang R, Jianjun L (2002) *Sinornis santensis* (Aves: Enantiornithes) from the

1086   Early Cretaceous of northeastern China. In: Chiappe LM, Witmer LM (eds) Mesozoic

1087   Birds: above the heads of dinosaurs. University of California Press, pp 184–208

1088   Sondaar PY (1977) Insularity and its effect on mammal evolution. In: Hecht MK, Goody PC,

1089   Hecht BM (eds) Major Patterns in Vertebrate Evolution. Springer US, pp 671–707

1090   Templeton AR (1983) Phylogenetic inference from restriction endonuclease cleavage site maps

1091   with particular reference to the evolution of humans and the apes. Evolution 37:221.

1092   Turner AH, Makovicky PJ, Norell MA (2012) A Review of Dromaeosaurid Systematics and

1093   Paravian Phylogeny. Bulletin of the American Museum of Natural History 371:1–206.

1094   Turner AH, Pol D, Clarke JA, Erickson GM, Norell MA (2007) A Basal Dromaeosaurid and

1095   Size Evolution Preceding Avian Flight. Science 317:1378–1381.

1096   Turner AH, Pol D, Norell MA (2011) Anatomy of *Mahakala omnogovae* (Theropoda:

1097   Dromaeosauridae), Tögrögiin Shiree, Mongolia. American Museum Novitates 1–66.

1098   Tykoski RS, Rowe TB (2004) Ceratosauria. In: Weishampel DB, Dodson P, Osmólska H (eds)

1099   The Dinosauria: Second Edition. University of California Press, pp 47–70

1100   van der Geer A, Lyras G, de Vos J, Dermitzakis M (2011) Evolution of island mammals:

1101   adaptation and extinction of placental mammals on islands. John Wiley & Sons,

1102   Chichester, UK

1103   Varricchio DJ, Chiappe LM (1995) A new enantiornithine bird from the Upper Cretaceous Two

1104   Medicine Formation of Montana. Journal of Vertebrate Paleontology 15:201–204.

1105   Vickers-Rich P, Chiappe LM, Kurzanov SM (2002) The enigmatic birdlike dinosaur *Avimimus*

1106   *portentosus*. In: Chiappe LM, Witmer LM (eds) Mesozoic Birds: above the heads of

1107   dinosaurs. University of California Press, pp 65–86

1108   Wagner GP, Gauthier J (1999) 1,2,3 = 2,3,4: A solution to the problem of the homology of the

1109   digits in the avian hand. Proceedings of the National Academy of Science USA. 96:5111–

1110   5116.

1111   Walker C, Dyke G (2009) Euenantiornithine birds from the Late Cretaceous of El Brete

1112   (Argentina). Irish Journal of Earth Sciences 27:15–62.

1113   Wang M, O'Connor JK, Zhou Z (2014a) A new robust enantiornithine bird from the Lower

1114   Cretaceous of China with scansorial adaptations. Journal of Vertebrate Paleontology

1115   34:657–671.

1116   Wang M, Zhou Z-H, O'Connor JK, Zelenkov NV (2014b) A new diverse enantiornithine family

1117   (Bohaiornithidae fam. nov.) from the Lower Cretaceous of China with information from

1118   two new species. Vertebrata Palasiatica 52:31–76.

1119   Welles SP (1984) *Dilophosaurus wetherilli* (Dinosauria, Theropoda). Osteology and

1120   comparisons. Palaeontographica Abteilung A A185:85–180.

1121   White MA, Falkingham PL, Cook AG, Hocknull SA, Elliott DA (2013) Morphological

1122   comparisons of metacarpal I for *Australovenator wintonensis* and *Rapator*

1123   *ornitholestoides*: implications for their taxonomic relationships. Alcheringa: An

1124   Australasian Journal of Palaeontology 37:435–441.

1125 Xu X, Choiniere JN, Pittman M, Tan Q, Xiao D, Li Z, Tan L, Clark JM, Norell MA, Hone DWE,
1126   Sullivan C (2010) A new dromaeosaurid (Dinosauria: Theropoda) from the Upper
1127   Cretaceous Wulansuhai Formation of Inner Mongolia, China. Zootaxa 2403:1–9.
1128 Xu X, Han F, Zhao Q (2014) Homologies and homeotic transformation of the theropod
1129   "semilunate" carpal. Scientific Reports 4:6042 doi: 10.1038/srep06042
1130 Xu X, Wang X-L (2003) A new dromaeosaur (Dinosauria:Theropoda) from the Early Cretaceous
1131   Yixian Formation of Western Liaoning. Vertebrata Pal Asiatica 42:111–119.
1132 Xu X, Wang X-L, Wu X-C (1999) A dromaeosaurid dinosaur with a filamentous integument
1133   from the Yixian Formation of China. Nature 401:262–266.
1134 Zanno LE (2010) A taxonomic and phylogenetic re-evaluation of Therizinosauria (Dinosauria:
1135   Maniraptora). Journal of Systematic Palaeontology 8:503–543.
1136 Zanno LE, Makovicky PJ (2011) Herbivorous ecomorphology and specialization patterns in
1137   theropod dinosaur evolution. PNAS 108:232–237.
1138 Zanno LE, Varricchio DJ, O'Connor PM, Titus AL, Knell MJ (2011) A New Troodontid
1139   Theropod, *Talos sampsoni* gen. et sp. nov., from the Upper Cretaceous Western Interior
1140   Basin of North America. PLoS ONE 6:e24487.
1141 Zhang Z, Chiappe LM, Han G, Chinsamy A (2013) A large bird from the Early Cretaceous of
1142   China: new information on the skull of enantiornithines. Journal of Vertebrate
1143   Paleontology 33:1176–1189.
1144 Zhang Z, Gao C, Meng Q, Liu J, Hou L, Zheng G (2009) Diversification in an Early Cretaceous
1145   avian genus: evidence from a new species of *Confuciusornis* from China. J Ornithol
1146   150:783–790.
1147 Zheng X, O'Connor JK, Huchzermeyer F, Wang X, Wang Y, Zhang X, Zhou Z (2014) New
1148   Specimens of *Yanornis* Indicate a Piscivorous Diet and Modern Alimentary Canal. PLoS
1149   ONE 9:e95036.
1150 Zhou S, Zhou Z, O'Connor J (2014) A new piscivorous ornithuromorph from the Jehol Biota.
1151   Historical Biology 26:608–618.
1152 Zhou Z-H, Zhang F (2002) A long-tailed, seed-eating bird from the Early Cretaceous of China.
1153   Nature 418:405–409.
1154 Zhou Z, Clarke J, Zhang F (2008) Insight into diversity, body size and morphological evolution
1155   from the largest Early Cretaceous enantiornithine bird. Journal of Anatomy 212:565–577.

1156   Zhou Z, Li FZZ (2010) A new Lower Cretaceous bird from China and tooth reduction in early

1157   avian evolution. Proceedings of the Royal Society of London B: Biological Sciences

1158   277:219–227.

1159   Zhou Z, Zhang F (2003) Anatomy of the primitive bird *Sapeornis chaoyangensis* from the Early

1160   Cretaceous of Liaoning, China. Canadian Journal of Earth Sciences 40:731–747.

1

Comparison between the scapulocoracoid of *Balaur* and other paravians.

Comparison of the scapulocoracoid of (A) *Balaur* (lateral view) to that of (B) the pygostylian *Enantiophoenix* (medial view); and (C) the dromaeosaurid *Velociraptor* (lateral view); (A) after Csiki et al. (2010, fig. 1); (B) modified after Cau and Arduini (2003, fig. 2); (C) after Norell and Makovicky (1999, fig. 4). All scapulocoracoids are drawn with the proximal half of the scapular blade oriented horizontally to show relative placement of coracoid tubercle. Scale bar: 10 mm (A); 5 mm (B); 10 mm (C). Abbreviations: ac, acromion; co, coracoid; ct, coracoid tubercle; gl, glenoid; me, missing element; sc, scapula; snf, supracoracoid nerve foramen.
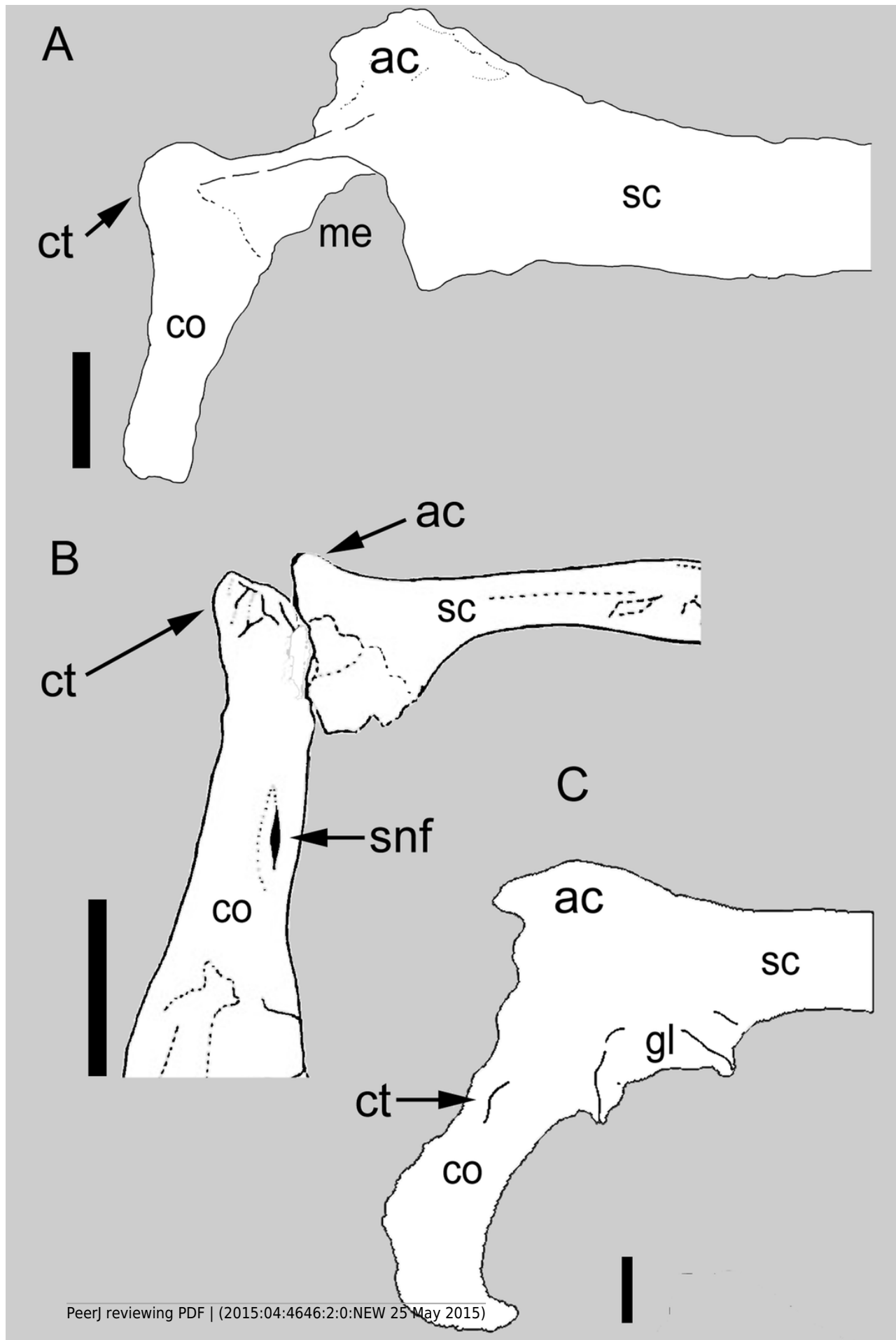
2

Comparison between the manus of *Balaur* and other paravians.

Comparison of the manus of (A) *Balaur* to those of (B) the enantiornithine *Zhouornis*; (C) the pygostylian *Sapeornis*; and (D) the dromaeosaurid *Deinonychus*, showing bird-like features of Balaur. (A) after Csiki et al. (2010, fig. 1, mirrored from original); (B) after Zhang et al. (2013, fig. 7); (C) after Zhou and Zhang (2003, fig. 7); (D) after Wagner and Gauthier (1999, fig. 2). All drawn at the same metacarpal II length. Scale bar: 20 mm (A, D); 10 mm (B, C). Abbreviations: cis, closed intermetacarpal space; cmc, carpometacarpus; d3, reduced third digit; drc, distally restricted condyles; lsc, laterally shifted semilunate carpal; p1-III, first phalanx of manual digit 3; p2-III, second phalanx of manual digit 3; pec, proximally expanded extensor surface; pnm, proximally narrow metacarpal I; U, ungual; usc, unfused semilunate carpal.
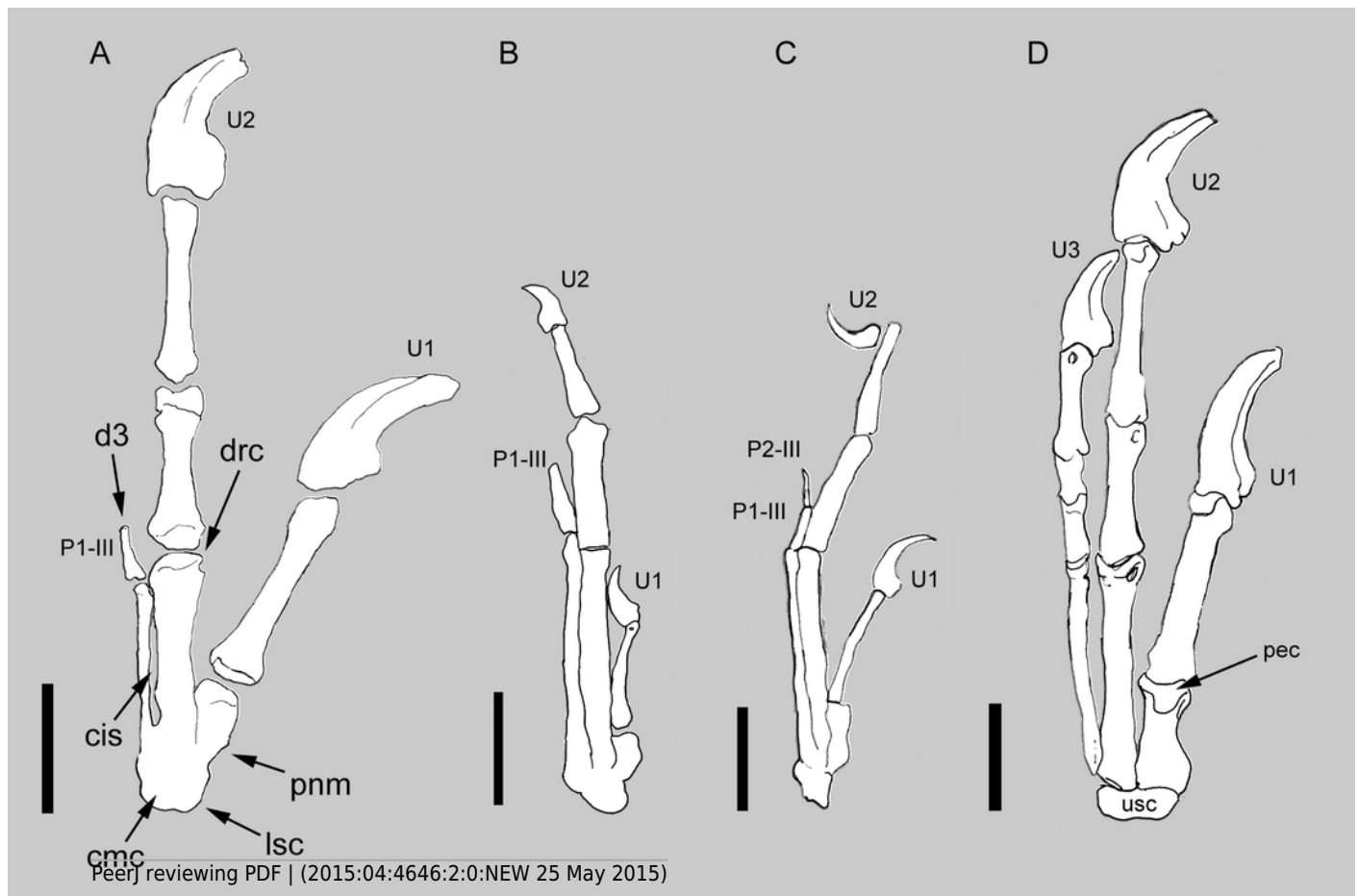
Comparison between the pelvis of *Balaur* and other paravians.

Pelvis of *Balaur* in lateral view (A). Comparison of the pubes of *Balaur* in anteroventral view (B) to those of the pygostylian *Sapeornis* in anterior view (C), and the dromaeosaurid *Velociraptor* in posterior view (D). (C) after Zhou and Zhang (2003, fig. 8); (D) after Norell and Makovicky (1999, fig. 19). Scale bar: 10 mm (A, B, D), 2 mm (C). Abbreviations: aa, antitrochanter; ac, acetabulum; cf, cuppedicus fossa; dfi, dorsal flange of ischium; ipf, interpubic fenestra; is, ischium; pa, pubic apron; ps, pubic symphysis; pu, pubis, sv, sacral vertebrae.
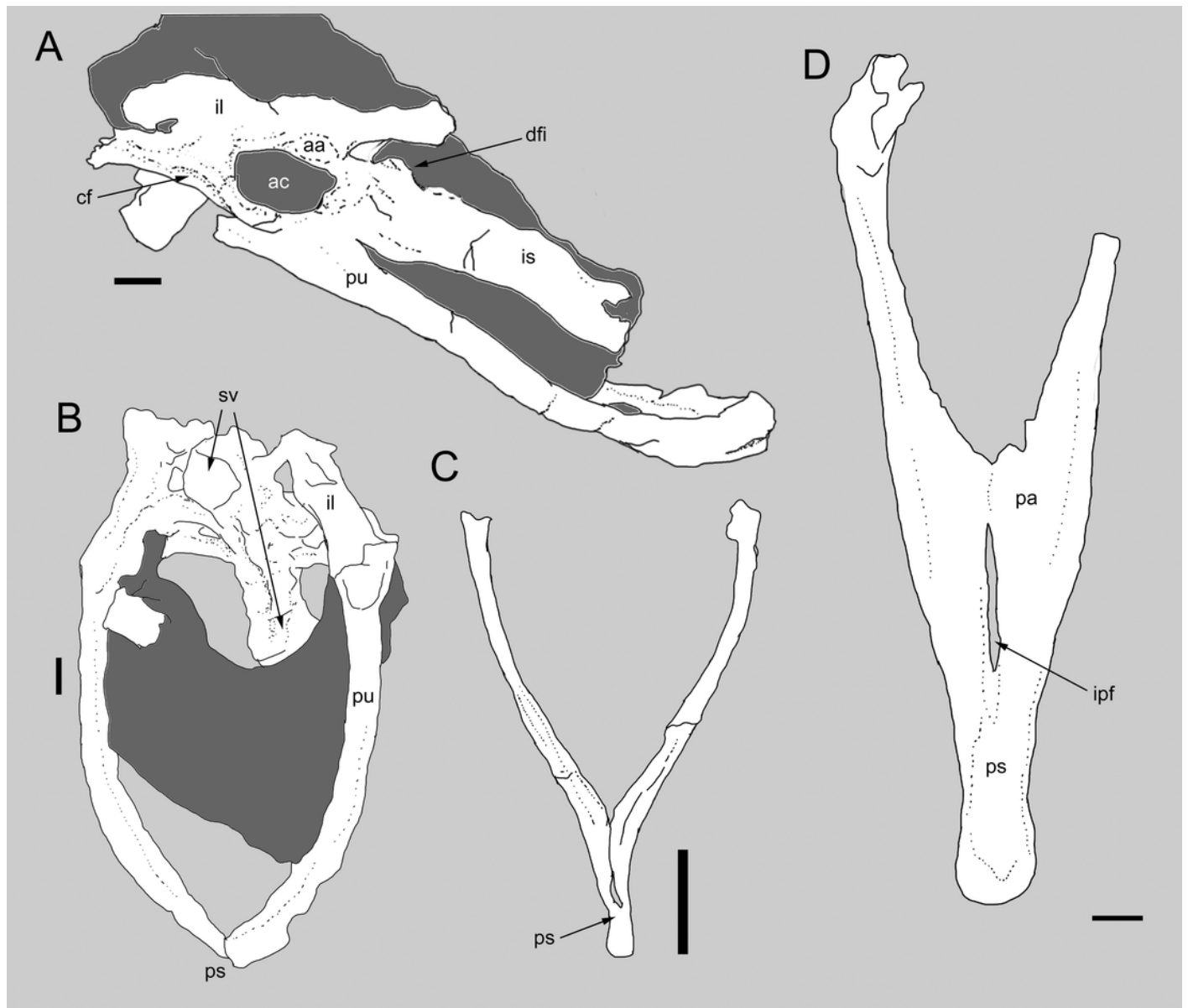
Comparison between the metatarsus of *Balaur* and other paravians.

Comparison of the metatarsus and pes of (B) *Balaur* to that of (A) the dromaeosaurid *Velociraptor*; and (C) the pygostylian *Zhouornis*. (a) after Norell and Makovicky (1997 figs. 6); (C) after Zhang et al. (2013, fig. 8, mirrored from original). Scale bar: 20 mm (A, B); 10 mm (C). Abbreviations: mt I, metatarsal I; mt V, metatarsal V; tt, tibiotarsus; U II: pedal ungual II; U IV, pedal ungual IV.
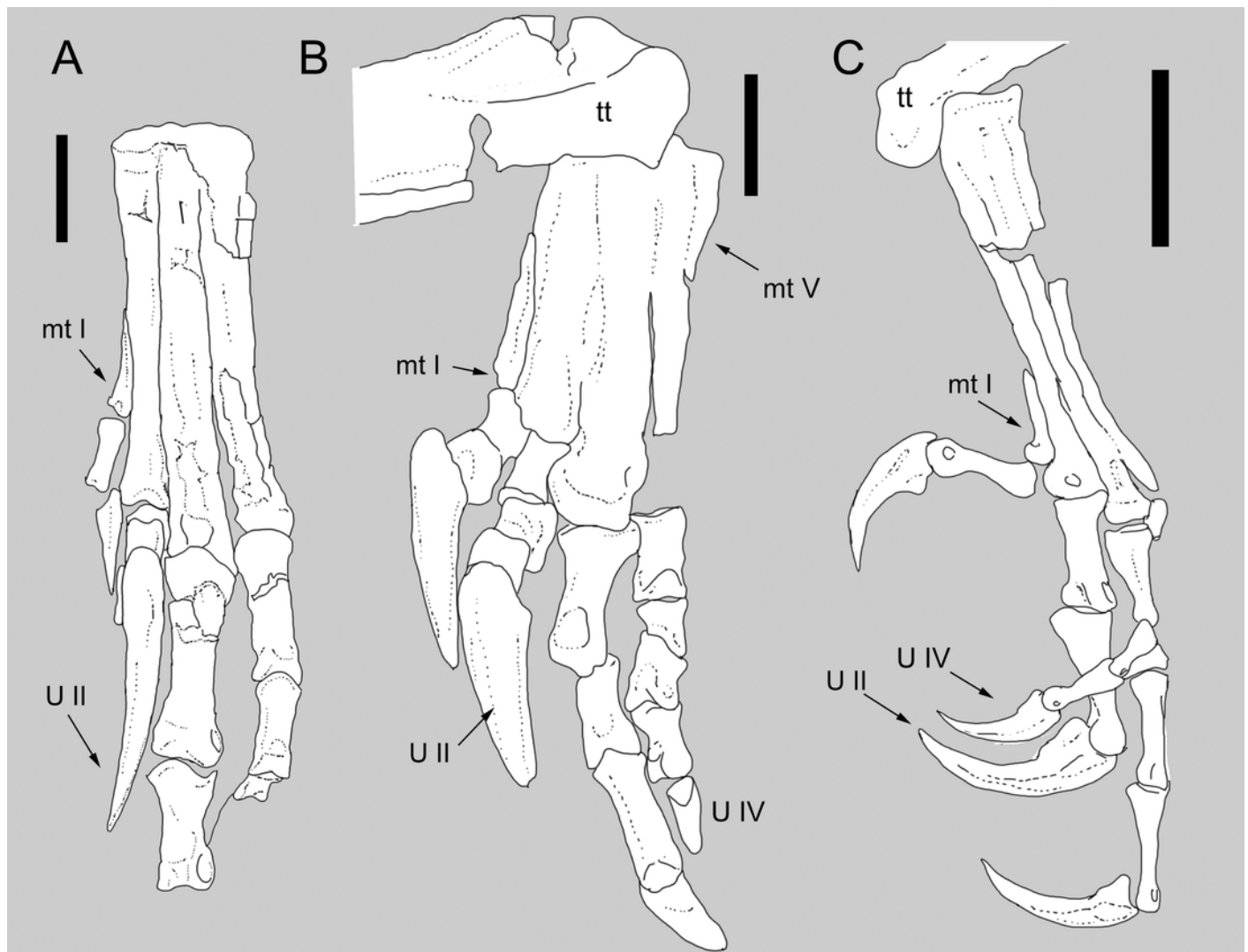
5

Updated dataset of Brusatte et al. (2014)

Reduced strict consensus of the shortest trees from the analysis of the modified Brusatte et al. (2014) matrix after pruning the 'wildcard' taxa *Epidendrosaurus*, *Hesperonychus*, *Kinnareemimus*, *Pedopenna*, *Pyroraptor*, and *Shanag*. Numbers adjacent to nodes indicate Decay Index values >1.

AVIALAE
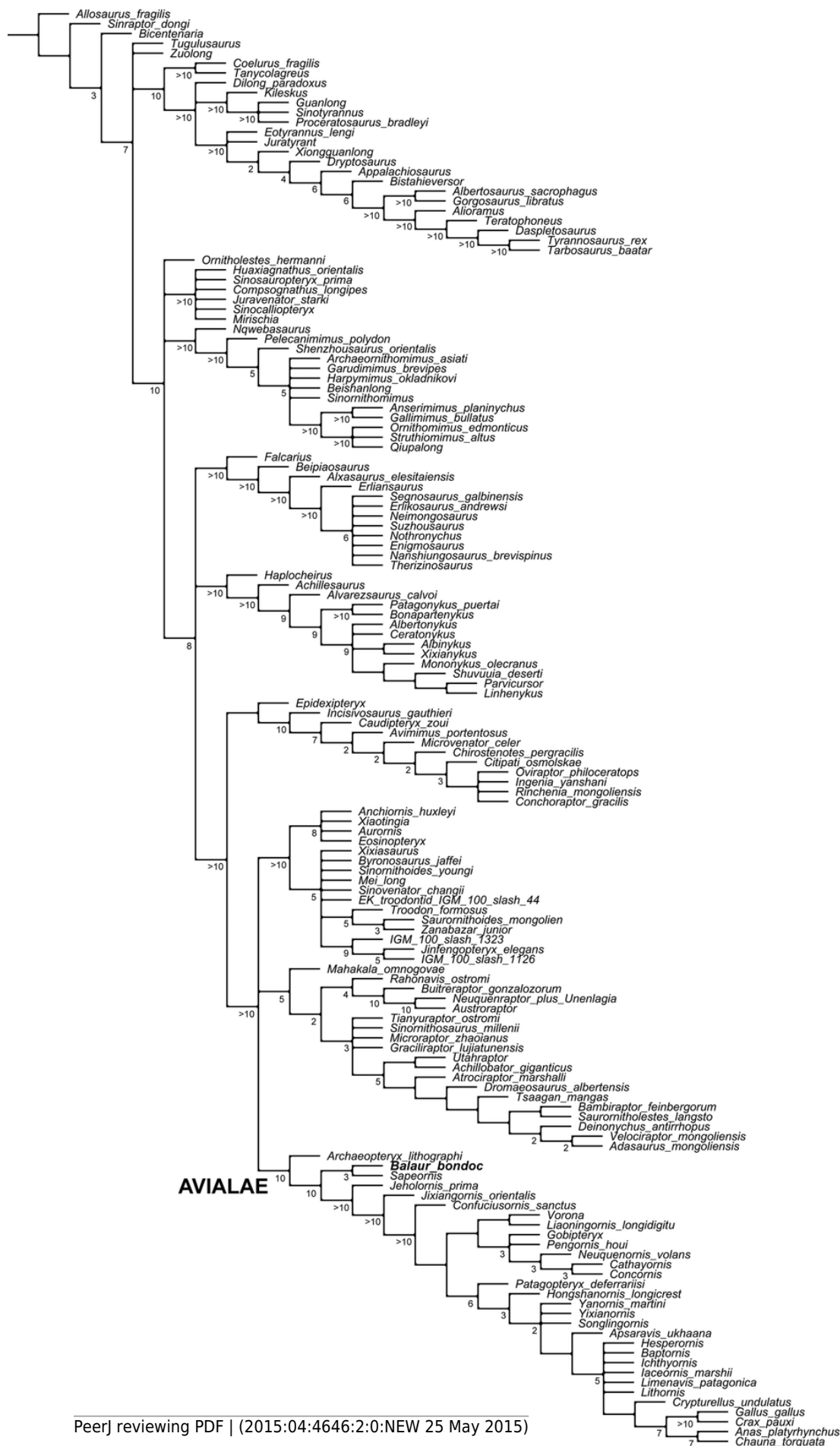
Updated dataset of Lee et al. (2014)

AVIALAE

7

Skeletal reconstruction of *Balaur*.

Speculative skeletal reconstruction for *Balaur bondoc*, showing known elements in white and unknown elements in grey. Note that the integument would presumably have substantially altered the outline of the animal in life. Produced by Jaime Headden, used with permission.